Syntheses and Crystal Structures of Disulfide-Bridged Binuclear Ruthenium Compounds: The First UV−Vis, Raman, ESR, and XPS Spectroscopic Characterization of a Valence-Averaged Mixed-Valent $Ru^{III}SSRu^{II}$ Core

Kazuko Matsumoto,*[1a] Takaya Matsumoto,[1a] Masaki Kawano,[1a] Hiroshi Ohnuki,[1a] Yushi Shichi,[1b] Toshikazu Nishide,[1c] and Toshio Sato[1d]

Contribution from the Department of Chemistry, Waseda University, Tokyo 169, Japan, Nissan ARC Ltd., 1, Natsushima, Yokosuka, Kanagawa 237, Japan, Central Engineering Laboratories, Nissan Motor Co. Ltd., 1, Natsushima, Yokosuka, Kanagawa 237, Japan, and Instrumental Analysis Center of Chemistry, Faculty of Science, Tohoku University, Aramaki Aoba, Aoba-ku, Sendai 980, Japan

Received February 6, 1995. Revised Manuscript Received September 11, 1995[⊗]

Abstract: Disulfide-bridged binuclear ruthenium complexes, $[\{RuCl(P(OMe)_3)_2\}_2(\mu\text{-}Cl)_2(\mu\text{-}S_2)]$ (**1**), $[\{RuCl(P(OMe)_3)_2\}(\mu\text{-}Cl)_2(\mu\text{-}S_2)\{Ru(CH_3CN)(P(OMe)_3)_2\}]^+$ (**[2]**$^+$), $[\{Ru(CH_3CN)_3(P(OMe)_3)_2\}_2(\mu\text{-}S_2)]^{3+}$ (**[3]**$^{3+}$), $[\{Ru(CH_3CN)(P(OMe)_3)_2\}_2(\mu\text{-}Cl)_2(\mu\text{-}S_2)]^{2+}$ (**[4]**$^{2+}$), and $[\{Ru(CH_3CN)_3(P(OMe)_3)_2\}_2(\mu\text{-}S_2)]^{4+}$ (**[5]**$^{4+}$), have been synthesized, and their crystal structures have been solved. Compounds **1**, **[2]**$^+$, and **[4]**$^{2+}$ have a triply bridged Ru^{III} $(\mu\text{-}Cl)_2(\mu\text{-}S_2)Ru^{III}$ core, in which the S_2^{2-} ligand bridges the two Ru atoms in a cis configuration. Compounds **[3]**$^{3+}$ and **[5]**$^{4+}$ have a singly bridged *trans*-RuSSRu core, whereby **[3]**$^{3+}$ corresponds to a one-electron reduced form of **[5]**$^{4+}$. Compound **[3]**$^{3+}$ is the first example of a well-characterized mixed-valent compound with a trans-MSSM core, where M is any metal. All the compounds have intense absorption bands at around 700 nm, which can be explained for **[3]**$^{3+}$ and **[5]**$^{4+}$ as a $\pi-\pi^*$ transition of the distinct *trans*-RuSSRu core. Resonance Raman spectroscopy of **1**, **[2]**$^+$, and **[3]**$^{3+}$ and comparison with several literature values for *cis*-RuSSRu compounds show that only **[3]**$^{3+}$ exhibits a strong ν(S−S) Raman band, when excited by $\lambda_e = 647.1$ nm, whereas all the others show strong to medium ν-(Ru−S) and very weak ν(S−S) bands. The ESR spectrum of **[3]**$^{3+}$ shows a rhombic signal with $g_1 = 2.12$, $g_2 = 2.05$, and $g_3 = 1.995$. This anisotropy is unusually small, compared to most mononuclear and binuclear Ru(III) compounds with various ligands. Analysis of the g values by use of the matrix of spin−orbit coupling Hamiltonian has revealed a very small spin−orbit coupling constant of 100 cm^{-1}, which is a result of the extensive covalency of the metal−disulfide bond. The X-ray photoelectron spectrum of **[3]**$^{3+}$ did not give any of the expected double peaks of the Ru(II) and Ru(III) components; the observed peaks are $Ru^{3d}{}_{5/2}$ 281.0 eV, $3P_{3/2}$ 462.4 eV, $S(S_2^{2-})$ $2P_{3/2}$ 162.7 eV. Compound **[3]**$^{3+}$ does not give any intervalence-transition band in the longer-wavelength visible to near-IR region, other than the UV−vis band similarly observed in the one-electron oxidized compound **[5]**$^{4+}$. These characteristics are reasonably understood, if **[3]**$^{3+}$ is regarded as a mixed-valent complex with valence-averaged ground state (class III of the Robin and Day classification).

Introduction

Transition-metal complexes with S^{2-} ligand are widely distributed in nature as ores and redox active centers in metalloenzymes such as ferridoxins or nitrogenases.[2−6] Other sulfur-containing ligands such as RS^-, HS^-, dithiocarbamates and other dithiochelates, and thiocrown ethers, have also been shown to exhibit novel redox nature, owing to the d orbitals and strongly donating nature of sulfur. Polysulfides (S_x^{2-}, $x \geq 2$) are known to act as chelating or bridging ligands to transition metals,[7] and above all S_2^{2-} is a remarkably strong electron donor among the other polysulfides (S_y, $y \geq 3$).[8,9]

We have attempted to synthesize sulfide-bridged multinuclear ruthenium compounds, whose core structures are robust against ligand substitution and subsequent ligand redox reactions, thus providing various catalytic redox functions. In our previous studies, trinuclear compounds, $[\{(P(OMe)_3)_4Ru\}_2(\mu\text{-}MS_4)](PF_6)_2$[10] (M = Mo, W) and $[\{(L)(CO)(PPh_3)Ru\}_2(\mu\text{-}MS_4)]$[11] (L = PhNCHS, $CH_2CH_2(C_5H_4N)$, $CH_2CH_2C(O)OMe$, M = Mo, W), were synthesized, and their chemical properties were studied. Although the compounds were found to exhibit novel photosubstitution reactions,[11] it turned out that the bridging MS_4^{2-} ligand is strongly electron-accepting, causing the redox potential of Ru(II/III) to shift to a higher value than those of the starting mononuclear Ru compounds. In order to lower the redox potential of such compounds, the ruthenium center must be more electron-rich. The disulfide ligand S_2^{2-} is noted as well as the S^{2-} for its strong electron-donating nature, which is

⊗ Abstract published in *Advance ACS Abstracts,* March 15, 1996.

(1) (a) Waseda University. (b) Nissan ARC Ltd. (c) Nissan Motor Co. (d) Tohoku University.

(2) Holm, R. H. *Chem. Soc. Rev.* **1981**, *10*, 455.

(3) Coucouvanis, D. *Acc. Chem. Rev.* **1981**, *14*, 201.

(4) Zumft, W. G. *Eur. J. Biochem.* **1978**, *91*, 345.

(5) Palermo, R. E.; Singh, R.; Bashkin, J. K.; Holm, R. H. *J. Am. Chem. Soc.* **1984**, *106*, 2600.

(6) Holm, R. H.; Simhon, E. D. In *Molybdenum Enzymes*; Spiro, T. G., Ed.; Wiley Interscience: New York, 1985; Chapter 1.

(7) Schmidt, M; Hoffmann, G. G. *Z. Naturforsch.* **1979**, *B34*, 451.

(8) Müller, A.; Jaegermann, W.; Enemark, J. H. *Coord. Chem. Rev.* **1982**, *46*, 245.

(9) Uemura, H.; Kawano, M.; Watanabe, T.; Matsumoto, T.; Matsumoto, K. *Inorg. Chem.* **1992**, *31*, 5137.

(10) Matsumoto, T.; Matsumoto, K.; Sato, T. *Inorg. Chim. Acta* **1992**, *202*, 31.

(11) Kato, M.; Kawano, M.; Taniguchi, H.; Funaki, M.; Moriyama, H.; Sato, T.; Matsumoto, K. *Inorg. Chem.* **1992**, *31*, 26.

0002-7863/96/1518-3597$12.00/0

exemplified in $[\{CpRu(PPh_3)_2\}_2(\mu\text{-}S_2)](BF_4)_2$[12] and 1,4-$[\{(MeCp)Ru(PPh_3)\}_2(\mu\text{-}S_2)_2]$[13] (Cp = cyclopentadienyl, MeCp = methylcyclopentadienyl). The ligand lowers remarkably the redox potential of the compounds. Several earlier workers noticed the unusual properties of a $Ru^{III}SSRu^{III}$ core including its intense blue-green color, strong Raman bands observable to higher progression, and unusually low redox potentials;[14,15] however, compounds with a RuSSRu core have been rare, and the electronic state of the RuSSRu core is still not fully understood.

We report here the syntheses, crystal structures, and spectroscopic properties of several diruthenium compounds with novel *cis*- and *trans*-Ru_2S_2 core structures: $[\{RuCl(P(OMe)_3)_2\}_2(\mu\text{-}Cl)_2(\mu\text{-}S_2)]$, $[\{RuCl(P(OMe)_3)_2\}(\mu\text{-}Cl)_2(\mu\text{-}S_2)\{Ru(CH_3CN)(P(OMe)_3)_2\}](CF_3SO_3)$, $[\{Ru(CH_3CN)(P(OMe)_3)_2\}_2(\mu\text{-}Cl)_2(\mu\text{-}S_2)](CF_3SO_3)_2$, and $[\{Ru(CH_3CN)_3(P(OMe)_3)_2\}_2(\mu\text{-}S_2)]^{n+}$ (n = 3 and 4). The last compound with $n = 3$ is the first paramagnetic ruthenium compound with a mixed-valent $Ru^{II}SSRu^{III}$ core, whose crystal structure and detailed spectroscopic properties are reported here. Since extensive electron delocalization between the ligand and the metals is expected,[14−16] it is of interest to examine (i) the extent of the electron delocalization between the metals and the bridging ligand, (ii) where in the core one unpaired spin of the Ru(III) actually resides, and (iii) to what extent the S_2^{2-} ligand mediates the electron delocalization between the two metals in terms of the mixed-valent classification proposed by Robin and Day.[17,18] The crystal structures of some of the complexes in the present paper have been briefly reported as preliminary letters.[19,20] The UV−vis absorption, ESR, X-ray photoelectron spectra (XPS), and the cyclic voltammetry of the RuSSRu core are reported in the present paper.

Experimental Section

All the preparations were carried out in air unless otherwise stated.

$[\{RuCl(P(OMe)_3)_2\}_2(\mu\text{-}Cl)_2(\mu\text{-}S_2)]$ (1). All of the solvents used for the preparation of **1** were dried with 4A molecular sieves before use. *trans*-$RuCl_2(P(OMe)_3)_4$[21] (0.67 g, 1 mmol) and sulfur powder (0.32 g, 10 mmol) were suspended in 50 mL of CH_2Cl_2 and were reacted at room temperature for 24 h. The solution was concentrated to 5 mL under reduced pressure, and 5 mL of acetone was added. The solution was filtered to remove unreacted sulfur. The acetone addition and filtration was repeated several times until all the unreacted sulfur had been removed. The filtrate was concentrated to 3 mL under reduced pressure, and ether was added until a green powder of **1** was precipitated. The precipitate was filtered and recrystallized from acetone/ether. The yield was 65%. Green needle-like crystals for X-ray diffraction were obtained by vapor diffusion of ether into the acetone solution. The compound is air-stable, being soluble in CH_2Cl_2 and most other organic solvents except ether and *n*-hexane. Anal. Calcd for $C_{12}H_{36}O_{12}P_4Cl_4S_2Ru_2$: C, 15.94; H, 4.01. Found: C, 15.82; H, 4.09. ^{1}H NMR ($CDCl_3$): δ 3.72 (t, J = 5.13 Hz) (this triplet may be actually an overlap of two doublets). $^{31}P\{^1H\}$ NMR ($CDCl_3$): δ 120.14 (s). $^{31}P\{^1H\}$ NMR ($CDCl_3$): δ 128.83 (s). FABMS: *m/e* 905 (M^+), 870 ($M^+ - Cl$), 836 ($M^+ - 2Cl$), 781 ($M^+ - TMP$), 744 ($M^+ - Cl - TMP$), 711 ($M^+ - 2Cl - TMP$), 587 ($M^+ - 2Cl - 2TMP$). UV−vis (CH_2Cl_2): λ_{max} 737 nm ($\epsilon = 9.21 \times 10^3$ M^{-1} cm^{-1}), 472 ($\epsilon = 3.46 \times 10^3$), 334 ($\epsilon = 4.35 \times 10^3$). UV−vis ($CH_3CN$): λ_{max} 735 nm ($\epsilon = 9.63 \times 10^3$ M^{-1} cm^{-1}), 471 ($\epsilon = 3.25 \times 10^3$), 333 ($\epsilon = 4.50 \times 10^3$).

$[\{RuCl(P(OMe)_3)_2\}(\mu\text{-}Cl)_2(\mu\text{-}S_2)\{Ru(CH_3CN)(P(OMe)_3)_2\}](PF_6)$ (2(PF_6)). To a CH_3CN solution (30 mL) of **1** (0.90 g, 1.0 mmol) was added an aqueous solution (120 mL) of $NaPF_6$ (0.34 g, 2.0 mol), and the solution was stirred at room temperature for 10 min (completion of the reaction cannot be checked visually, so it is necessary to monitor the reaction with a UV−vis spectrometer). To the solution was added 150 mL of CH_2Cl_2, which formed a green organic layer and an aqueous layer. The organic layer was collected by using a separatory funnel and was filtered and condensed to 5 mL. Green thin plate crystals of **2(PF_6)** were obtained by ether vapor diffusion to the solution at room temperature. Rhombic block crystals were obtained by ether vapor diffusion into a CH_2Cl_2 solution of the isolated compound in a refrigerator; however, the crystals obtained were unstable in X-ray irradiation, and the X-ray structural analysis could not be carried out. Compound **2(PF_6)** is stable in air and is soluble in CH_2Cl_2, most organic solvents, and water but is insoluble in ether and hexane. The yield was 61%. Anal. Calcd for $C_{14}H_{39}NO_{12}F_6P_5Cl_3S_2Ru_2$: C, 15.94; H, 3.73; N, 1.33. Found: C, 16.16; H, 3.68; N, 1.42. ^{1}H NMR (CD_3CN): δ 3.72 (d, $^3J_{P-H}$ = 4.62 Hz), 3.674 (d, $^3J_{P-H}$ = 4.62 Hz). $^{31}P\{^1H\}$ NMR (CD_3CN): δ 124.28 (s), 114.47 (s), −145.62 (septet, $^1J_{F-P}$ = 706.2 Hz). UV−vis (CH_2Cl_2): λ_{max} 689 nm ($\epsilon = 7.93 \times 10^3$ M^{-1} cm^{-1}), 448 ($\epsilon = 2.30 \times 10^3$), 312 ($\epsilon = 4.05 \times 10^3$). UV−vis ($CH_3CN$): λ_{max} 690 nm ($\epsilon = 8.70 \times 10^3$ M^{-1} cm^{-1}), 450 ($\epsilon = 2.77 \times 10^3$), 313 ($\epsilon = 4.72 \times 10^3$).

$[\{RuCl(P(OMe)_3)_2\}(\mu\text{-}Cl)_2(\mu\text{-}S_2)\{Ru(CH_3CN)(P(OMe)_3)_2\}](CF_3SO_3)$ (2(CF_3SO_3)). The compound was prepared in the same way as for **2(PF_6)** by using $NaCF_3SO_3$ instead of $NaPF_6$. Green plate crystals obtained by ether vapor diffusion into the CH_2Cl_2 solution of **2(CF_3SO_3)** were suitable for X-ray diffraction analysis. The compound can also be prepared by addition of 1 equiv of $AgCF_3SO_3$ to the CH_3CN solution of **1**. The solution was stirred at room temperature for 3 h, filtered to remove AgCl, and condensed under vacuo, to which ether was added to precipitate **2(CF_3SO_3)**. Anal. Calcd for $C_{15}H_{39}NO_{15}Cl_3F_3P_4S_3Ru_2$: C, 17.01; H, 3.71; N, 1.32. Found: C, 17.07; H, 4.13; N, 1.57. UV−vis (CH_2Cl_2): λ_{max} 689 nm ($\epsilon = 7.93 \times 10^3$ M^{-1} cm^{-1}), 448 ($\epsilon = 2.30 \times 10^3$), 312 ($\epsilon = 4.05 \times 10^3$).

$[\{Ru(CH_3CN)_3(P(OMe)_3)_2\}_2(\mu\text{-}S_2)](PF_6)_3$ (3(PF_6)$_3$). To a CH_3CN solution (50 mL) of **1** (0.90 g, 1.0 mmol) was added an aqueous solution (120 mL) of $NaPF_6$ (1.01 g, 6.0 mmol) in a N_2 atmosphere, and the solution was stirred at room temperature for 3 h. During this time the green solution turned blue. To the solution was added 150 mL of CH_2Cl_2, and the blue organic layer was separated from the aqueous layer. The organic layer was filtered and condensed to 10 mL. Blue plate crystals were obtained by ether vapor diffusion to the organic solution in a refrigerator. The crystal is dichroic, being red or green depending on the direction of observation. Compound **3(PF_6)$_3$** is not very stable in air and is very soluble in CH_3CN but sparingly soluble in CH_2Cl_2. The compound is also soluble in most organic solvents except $CHCl_3$, ether, and hexane; however, the blue color changes even under N_2 in these solvents. The yield was 72%. Anal. Calcd for $C_{24}H_{54}N_6O_{12}F_{18}P_7S_2Ru_2$: C, 19.97; H, 3.77; N, 5.82. Found: C, 19.92; H, 3.67; N, 5.84. ^{1}H NMR (CD_3CN): δ 3.79 (t, J = 5.45 Hz) (this triplet may actually be an overlap of two doublets), 6.33 (broad). $^{31}P\{^1H\}$ NMR (CD_3CN): δ −145.61 (septet, $^1J_{F-P}$ = 706.5 Hz). The ^{31}P NMR signal of $P(OMe)_3$ cannot be observed, because **[3]**$^{3+}$ is paramagnetic. UV−vis (CH_3CN): λ_{max} 646 nm ($\epsilon = 6.36 \times 10^3$ M^{-1} cm^{-1}), 317 ($\epsilon = 2.84 \times 10^3$), 256 ($\epsilon = 15.63 \times 10^3$).

$[\{Ru(CH_3CN)_3(P(OMe)_3)_2\}_2(\mu\text{-}S_2)](CF_3SO_3)_3$ (3(CF_3SO_3)$_3$). The compound is prepared similarly to the PF_6^- salt, by using $NaCF_3SO_3$ in place of $NaPF_6$. The yield was 70%. The compound can also be prepared by stirring a CH_3CN solution containing **1** and **4** equiv of $AgCF_3SO_3$ at room temperature for 3 h. The solution was filtered, and the filtrate was condensed under vacuo, to which ether was added to precipitate **3(CF_3SO_3)$_3$** with a yield of 82%. Anal. Calcd for $C_{27}H_{54}N_6O_9F_9P_4S_5Ru_2$: C, 22.27; H, 3.74; N, 5.77. Found: C, 22.15; H, 3.80; N, 5.63.

$[\{Ru(CH_3CN)(P(OMe)_3)_2\}_2(\mu\text{-}S_2)(\mu\text{-}Cl)_2](CF_3SO_3)_2$ (4). All the procedures described below should be carried out under dry N_2. To a dry CH_3CN solution (8 mL) of **1** (0.1 g, 0.11 mmol) was added 2 equiv

(12) Amarasekera, J.; Rauchfuss, T. B.; Wilson, R. S. *Inorg. Chem.* **1987**, *26*, 3328.
(13) Amarasekera, J.; Rauchfuss, T. B.; Rheingold, A. L. *Inorg. Chem.* **1987**, *26*, 2017.
(14) Elder, R. C.; Trkula, M. *Inorg. Chem.* **1977**, *5*, 1048.
(15) Kim, S.; Otterbein, E. S.; Rava, R. P.; Isied, S. S.; Filippo, J. S., Jr.; Waszcyak, J. V. *J. Am. Chem. Soc.* **1983**, *105*, 336.
(16) Sellmann, D.; Lechner, P.; Knoch, F.; Moll, M. *J. Am. Chem. Soc.* **1992**, *114*, 922.
(17) Robin, M. B.; Day, P. *Adv. Inorg. Chem. Radiochem.* **1967**, *10*, 247.
(18) Hush, N. S. *Prog. Inorg. Chem.* **1967**, *8*, 391.
(19) Matsumoto, T.; Matsumoto, K. *Chem. Lett.* **1992**, 559.
(20) Matsumoto, T.; Matsumoto, K. *Chem. Lett.* **1992**, 1539.
(21) Sime, W. J.; Stephenson, T. A. *J. Organomet. Chem.* **1978**, *161*, 245.

Table 1. Crystallographic Data

	1	**2(CF_3SO_3)**	**3(PF_6)$_3$**	**4**	**5**
formula	$C_{12}H_{36}O_{12}Cl_4P_4S_2Ru_2$	$C_{15}H_{39}NO_{15}Cl_3F_3P_4S_3Ru_2$	$C_{24}H_{54}N_6O_{12}F_{18}P_7S_2Ru_2$	$C_{18}H_{42}N_2O_{18}Cl_2F_6P_4S_4Ru_2$	$C_{28}H_{54}N_6O_{24}F_{12}P_4S_6Ru_2$
fw	904.38	1059.04	1443.77	1213.79	1605.14
cryst. system	monoclinic	orthorhombic	triclinic	monoclinic	monoclinic
space group	$P2_1/c$ (No. 14)	*Pnma* (No. 62)	*P*1 (No. 2)	$P2/a$ (No. 13)	$P2_1/c$ (No. 14)
a (Å)	23.739(8)	17.483(5)	12.469(3)	16.615(4)	21.984(6)
b (Å)	15.665(4)	29.964(5)	13.427(4)	20.182(5)	13.630(3)
c (Å)	8.794(1)	15.270(2)	11.834(3)	13.787(5)	21.531(6)
α (deg)	90.0	90.0	121.12(2)	90.0	90.0
β (deg)	99.93(2)	90.0	70.06(2)	92.75(2)	95.81(2)
γ (deg)	90.0	90.0	123.64(2)	90.0	90.0
V (Å^3)	3221(2)	8000(3)	1408.0(8)	4618(2)	6408(3)
T (deg)	23 ± 1	23 ± 1	23 ± 1	23 ± 1	23 ± 1
Z	4	8	1	4	4
ρ_{calcd} (g cm^{-3})	1.86	1.76	1.70	1.75	1.66
crystal dimens (mm)	0.51 × 0.10 × 0.12	0.45 × 0.20 × 0.15	0.50 × 0.38 × 0.13	0.47 × 0.35 × 0.12	0.74 × 0.25 × 0.13
absorp coeff (cm^{-1})	16.21	13.17	9.12	11.56	8.60
2*θ* range (deg)	$5 < 2\theta < 55$	$4 < 2\theta < 50$	$2 < 2\theta < 55$	$5 < 2\theta < 55$	$3 < 2\theta < 50$
no. of total data measd	6738	7745	8527	5743	12451
no. of obsd unique data	3053(4σ)	3402(4σ)	4023(4σ)	2497(4σ)	4033(4σ)
residual electron density (e/Å^3)	0.62	0.89	0.83	0.81	2.7
no. of params	324	422	450	217	389
R^a	0.0395	0.0859	0.0815	0.0803	0.1425
$R_w{}^b$	0.0502	0.0734	0.0697	0.0881	0.1431
w	$1/\sigma^2(F)$	$1/(\sigma^2(F) + 0.000512F^2)$	$1/\sigma^2(F)$	$1/\sigma^2(F)$	$1/(\sigma^2(F) + 0.002433F^2)$

[a] $R = \sum(|F_o| - |F_c|)/\sum|F_o|$. [b] $R_w = [\sum w(|F_o| - |F_c|)^2/\sum w|F_o|^2]^{1/2}$.

of $AgCF_3SO_3$, and the solution was stirred at room temperature for 3 h. The blue-green solution was filtered, and the filtrate was set aside for crystallization by ether vapor diffusion. The crystals were collected by filtration, washed with ether, and dried under vacuo. Blue plate crystals were obtained in a yield of 74%. Anal. Calcd for $C_{18}H_{42}N_2O_{18}Cl_2F_6P_4S_4Ru_2$: C, 17.81; H, 3.49; N, 2.31. Found: C, 17.78; H, 3.48; N, 2.59. $^{31}P\{^1H\}$ NMR (CD_3CN): δ 117 ($\nu_{1/2} = 360$ Hz). UV−vis (CH_3CN): λ_{max} 664 nm ($\epsilon = 7.50 \times 10^3$ M^{-1} cm^{-1}), 419 ($\epsilon = 1.85 \times 10^3$), 315 ($\epsilon = 3.99 \times 10^3$).

[{Ru(CH_3CN)$_3$($P(OMe)_3$)$_2$}$_2$(μ-S_2)](CF_3SO_3)$_4$ (5). All the procedures described in the following must be carried out under dry N_2. To a dry CH_3CN solution (2 mL) of **1** (0.1 g, 0.11 mmol) was added 4 equiv of $AgCF_3SO_3$ (0.104 g), and the solution was stirred at 50 °C for 40 h. After the solution was cooled, AgCl was removed by filtration, and the filtrate was dried under vacuo. The residue was dissolved in 10 mL of CH_2Cl_2 and was filtered. Ether vapor was introduced into the solution, which precipitated blue plate crystals of **5**. Compound **5** is very unstable in air and must be kept under dry N_2. The yield was 80%. Anal. Calcd for $C_{28}H_{54}N_6O_{24}F_{12}P_4S_6Ru_2$: C, 20.95; H, 3.39; N, 5.24. Found: C, 21.09; H, 3.49; N, 5.16. $^{31}P\{^1H\}$ NMR (CD_3CN): δ 112.3 ppm. UV−vis (CH_3CN): λ_{max} 652 nm ($\epsilon = 7.08 \times 10^3$ M^{-1} cm^{-1}), 310 ($\epsilon = 2.84 \times 10^3$).

Physical Measurements. Infrared spectra were recorded on a HITACHI I-3000 instrument, while UV−vis spectra were measured on Shimadzu UV-310PC and Shimadzu UV-260 spectrophotometers. Acetonitrile for the spectral measurements was dried with 4A molecular sieves and distilled before use. NMR spectra were recorded on JEOL GSX400 and JEOL EX-270 instruments. The ^{31}P chemical shifts are expressed in ppm, which is referenced to $P(OMe)_3$ in CD_3CN set at 140.0 ppm. ESR spectra were recorded on a JEOL JES-RE2X spectrometer using microcrystalline samples and CH_3CN solutions. Resonance Raman spectra were measured on a Spex Ramlog 6 double monochromator. The excitation sources were 647.1-nm and 568.2-nm lines of a Kr^+ laser and 476.5-nm line of an Ar^+ laser. FAB mass spectra were obtained on a JEOL JMS-HX110 instrument. The samples were measured as nitrobenzyl alcohol solutions. Cyclic voltammograms were measured by using a Fuso 315A potentiostat. A three-electrode system was employed with a Pt plate working electrode, a Pt wire counterelectrode, and an Ag/Ag^+ or Ag/AgCl reference electrode. The reference electrode was separated from the sample solutions via a Vycor glass junction. The CH_3CN used as solvent was dried with 4A molecular sieves and distilled. Tetrabutylammonium perchlorate (TBAP) was used as electrolyte.

The X-ray photoelectron spectra (XPS) were recorded on a Perkin-Elmer Model 5600 spectrometer. Mg Kα radiation (1253.6 eV) operated at 15 kV and 13.3 mA was used as an X-ray excitation source. Microcrystalline samples were dispersed on indium films and were used for measurement. Since C 1s peaks overlap on Ru $3d_{3/2}$ peaks, conventional calibration method of using the C 1s peak of hydrocarbon contaminant in air could not be used. As an alternative, the C 1s binding energy (286.1 eV) of the methoxy group in the ruthenium complexes was used for calibration of the binding energy. The carbon 1s binding energies of the methoxy group in over 50 compounds are reported to vary only in the range of 286.0−286.2 eV[22] and therefore would not give rise to any serious errors, if this peak is used as a standard of the binding energies. The reproducibility of the measurements was ±0.1 eV. Under these conditions, the Ag $3d_{5/2}$ peak had a full width at half maximum (FWHM) of 1.00 eV. All the sample preparations and mountings were carried out in a glovebox filled with Ar, directly connected to the sample chamber of the spectrometer.

Collection and Reduction of X-ray Data. Crystals of **1**, **2(CH_3SO_3)**, **3(PF_6)$_3$**, **4**, and **5** were subjected to single-crystal X-ray diffraction analysis. Unit cell parameters were obtained from a least-squares fit of 20 reflections in the range $20° < 2\theta < 25°$, measured on a Rigaku AFC-5R four-circle diffractometer by using graphite-monochromated Mo Kα radiation (0.710 68 Å). Since **4** and **5** are unstable in air, the crystal of **4** was coated with epoxy-resin and was used for X-ray measurement, whereas a crystal of **5** was sealed in a glass capillary under a N_2 atmosphere. No serious deterioration of the crystal was observed for **4** during the measurement, whereas about 10% intensity decay was observed for the three standard reflections of **5**, and therefore a decay correction was applied. An analytical absorption correction was applied according to the literature method.[23] The Lorentz−polarization correction was made to the collected data for all the crystals. The details of the crystal data and the data collections for **1**, **2(CF_3SO_3)**, **3(PF_6)$_3$**, **4**, and **5** are given in Table 1 and in Tables S1, S2, S3, S4, and S5, respectively, in the supporting information.

Solution and Refinement of the Structures. The coordinates of the metals and the coordinating atoms were determined by a direct

(22) Shichi, Y. Ph.D. Thesis, Keio University, Japan, 1990, p 50.
(23) North, A. T. C.; Phillips, D. C.; Mathews, F. S. *Acta Crystallogr.* **1968**, *A24*, 351.

Scheme 1

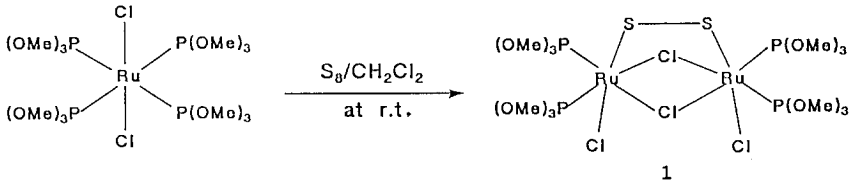

Scheme 2

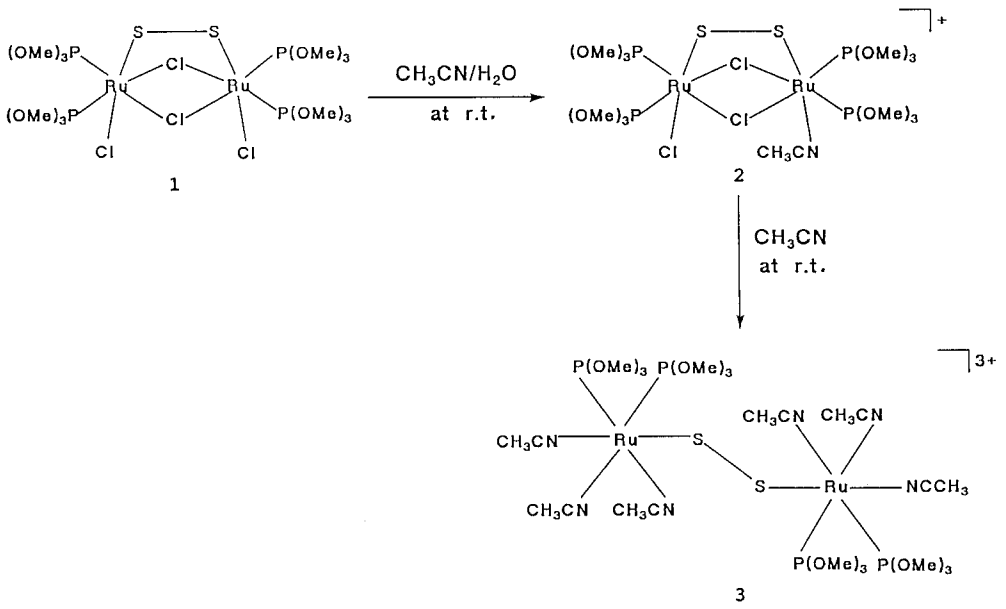

method (SHELXS86[24]). The subsequent Fourier synthesis and the block-diagonal least-squares refinement with program system UNICS-III[25] (**1** and **3(PF$_6$)$_3$**) or the full-matrix least-squares refinement with SHELX76/86 (**2(CF$_3$SO$_3$)**, **4**, and **5**) revealed all the non-hydrogen atoms, which were finally refined with anisotropic temperature factors to the final discrepancy indices listed in Table 1 ($R = \sum||F_o| - |F_c||/\sum|F_o|$ and $R_w = [\sum w_i(|F_o| - |F_c|)^2/\sum w_i|F_o|^2]^{1/2}$). Since the crystal of **5** is very unstable toward air and X-ray, it deteriorated significantly during the measurement. Only Ru, S, and P atoms of **5** could be refined anisotropically, while all other non-hydrogen atoms were refined isotropically.

In the intermediate stage of the X-ray analysis for **3(PF$_6$)$_3$**, all the non-hydrogen atoms were located with Fourier synthesis and were refined isotropically by the block-diagonal least-squares program (UNICS-III[25]). At this stage, some of the methoxy groups were found to be disordered in two positions (O13 vs O14, C13 vs C14, and O21−O23 vs O24−O26), and all the fluorine atoms of the hexafluorophosphate ions were also disordered in two positions (F11−F13 vs F14−F16, and F21−F26 vs F27−F212). The relative statistical weights of the two positions were determined by a full-matrix least-squares refinement (SHELX86) to be 62.37:37.63 for the methoxy groups and 56.78:43.22 for the fluorine atoms. All the atoms were finally refined with anisotropic temperature factors.

In the analysis of **2(CF$_3$SO$_3$)**, a crystallographically independent $CF_3SO_3^-$ anion was found to be distributed over two equivalent special positions (x, 0.25, z) with 0.5 multiplicity. Some of the bond distances in the $CF_3SO_3^-$ are not as normal (Table S18), but these are due to a large thermal motion of the anion.

The coordinates of the atoms in **1**, **2(CF$_3$SO$_3$)**, **3(PF$_6$)$_3$**, **4**, and **5** are listed in Tables S6, S7, S8, S9, and S10, respectively, in the supporting information. The anisotropic temperature factors are reported in the supporting information (Tables S11, S12, S13, S14, and S15, respectively).

Analysis of the ESR Spectrum. The powder ESR spectrum of **3-(PF$_6$)$_3$** was analyzed on the basis of the theory of the g tensors for low-spin d^5 systems in distorted octahedral environments, developed by Bleaney and O'Brien,[26] Stevens,[27] and Kamimura.[28] The theory has been successfully applied to monomeric low-spin Ru(III) complexes,[29] and the basic equations are outlined in the Appendix.

In the actual calculation, a home-made computer program was created, and g_x, g_y, and g_z values were calculated by varying the parameters in the following ranges: $\Delta = -250$, -500, and -1000 to -7000 cm^{-1} with -1000 increment; $V = \pm250$, ±500, ±1000, ±2000, and ±3000 cm^{-1}; $\lambda = \pm1000$, ±900, ±800, ±700, ±600, ±500, ±400, ±300, ±200, ±100, ±50, and 0 cm^{-1}; $k = 0.3-1.1$ with an increment of 0.1, where Δ and V are axial and rhombic distortion energy, λ is a spin−orbit coupling constant, and k is an orbital reduction factor. All combinations of these parameters were calculated, and the best parameters found were further refined by varying them by 10 cm^{-1} around the best value obtained by the first approximate survey. In the next survey, k was varied from 0.8 to 1.0 by an increment of 0.01.

Results and Discussion

Syntheses of the Complexes. From the reaction of *trans*-$RuCl_2(P(OMe)_3)_4$ with elemental sulfur, compound **1** was obtained (Scheme 1). No reaction occurred when the synthesis of **1** was attempted under a N_2 atmosphere.

Synthesis of **2** requires trace amounts of water, as shown in Scheme 2, and the reaction is accelerated by increasing the amount of the water. Substitution of the chloride in $RuCl_2(bpy)_2$ (bpy = bipyridine) by CH_3CN is reported to be similarly accelerated, with the mechanism involving initial hydrolysis of the complex.[30] Since the reaction of **[2]**$^+$ to **[3]**$^{3+}$ is slower than that of **1** to **[2]**$^+$, compound **2** can be isolated by terminating the reaction on addition of CH_2Cl_2 and isolating the organic

(24) SHELX86 by G. Sheldrick.
(25) Sakurai, T.; Kobayashi, K. *Rigaku Kenkyusho Hokoku* **1979**, *55*, 69.
(26) Bleaney, B.; O'Brien, M. C. M. *Proc. Phys. Soc.* **1956**, *69*, 1216.
(27) Stevens, K. *Proc. R. Soc. London, Ser. A* **1953**, *219*, 542.
(28) Kamimura, H. *J. Phys. Soc. Jpn.* **1956**, *11*, 1171.
(29) (a) Hudson, A.; Kennedy, M. J. *J. Chem. Soc. A* **1969**, 116. (b) Lahiri, G. K.; Bhattacharya, S.; Ghosh, B. K.; Chakravorty, A. *Inorg. Chem.* **1987**, *26*, 4324.
(30) Greaney, M. A.; Coyle, C. L.; Harmer, M. A.; Jordan, A.; Stiefel, E. I. *Inorg. Chem.* **1989**, *28*, 912.

Scheme 3

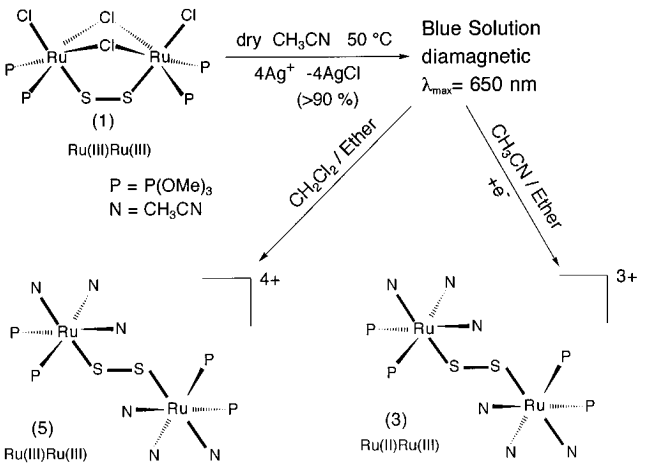

layer. The reaction of **1** to **[2]**$^+$ was monitored with UV−vis spectroscopy (Figure S1), which shows isosbestic points at 322, 361, 403, 456, 539, and 704 nm. The reaction is accelerated by small amounts of H_2O, probably because the increased polarity of the solvent facilitates the release of the coordinated chloride. Compound **[3]**$^{3+}$ has a mixed-valent $[Ru^{II}SSRu^{III}]^{3+}$ core, which corresponds to the one-electron reduced form of **[5]**$^{4+}$. The reduction of **[2]**$^+$ to **[3]**$^{3+}$ is caused by CH_3CN and not by H_2O, since the reduction reaction takes place even in dry CH_3CN as described in the preparation of **3(CF$_3$SO$_3$)$_3$** and is shown in Scheme 3. Scheme 3 shows that addition of 4 equiv of $AgCF_3SO_3$ to **1** removes more than 90% of the Cl^- in **1** as AgCl (confirmed gravimetrically). Addition of dry ether to the dry CH_3CN filtrate gives **[3]**$^{3+}$, whereas addition of dry ether to a dry CH_2Cl_2 solution containing the dried residue of the dried CH_3CN filtrate gives **[5]**$^{4+}$. In CD_3CN, the reduction of **[5]**$^{4+}$ is considerably retarded, and **5** can be isolated by ether addition. The UV−vis spectrum of **5** in CH_3CN gradually changes to that of **[3]**$^{3+}$ even under dry N_2 (see Figure 7 in the latter section). All these facts suggest that CH_3CN is the reducing agent for **[5]**$^{4+}$; however, we could not identify the oxidized product of CH_3CN. CH activation of CH_3CN to bridge two lanthanoid metals[31] and $NCCH_2^-$ coordination to square-planar late transition metals[32] are known, but redox reaction of CH_3CN with a metal ion is not known to the best of our knowledge. The detailed mechanism is still under investigation. Another disulfide-bridged $Ru^{II}SSRu^{III}$ dimer $[\{CpRu(PPh_3)_2\}_2(\mu\text{-}S_2)]^+$ has been isolated as its SbF_6^- salt;[12] however neither structure nor detailed spectroscopic study of the complex has been reported. All the compounds reported here are diamagnetic except **[3]**$^{3+}$, which is paramagnetic. All these magnetic properties were confirmed by NMR and ESR in the temperature range of room temperature to 77 K. It is noteworthy that addition of Cl^- sources such as R_4NCl to a CH_3CN solution of **[3]**$^{3+}$ in air or to an CH_3CN solution of **5** in N_2 restores the starting material **1**.

Structure of 1. The structure of **1** is shown in Figure 1. The two ruthenium atoms are bridged by a disulfide and two chloride ligands to form a novel $Ru_2(S_2)Cl_2$ core. Each ruthenium atom is further coordinated by a terminal chloride and two $P(OMe)_3$ ligands. The major atomic distances and angles in **1** are listed in Tables 2 and 3, respectively. All the interatomic distances and angles are tabulated in Tables S16 and S17, respectively, in the supporting information. The Ru−S−S angle is 111.4° on average (Table 3) and is within the normal value for end-on cis disulfide-bridged Ru dimer compounds (111.0−116.6°).[33,34] Table 4 summarizes the Ru−S and S−S distances and other spectroscopic properties of end-on cis and trans disulfide-bridged Ru dimer complexes so far reported. The S−S distance in **1** is one of the shortest of all the cis and trans disulfide bridges. The Ru−P distances in **1** (2.248(3), 2.242(3), 2.258(2), and 2.252(2) Å) are comparable to Ru^{III}−P($P(OMe)_3$) distances of 2.289(7), 2.275(8), 2.294(6), and 2.271(5) Å in $[\{Ru(P(OMe)_3)_4\}_2(\mu\text{-}WS_4)](PF_6)_2$,[10] but are significantly shorter than the Ru^{III}−P distances of other alkyl- or arylphosphine compounds ($[CpRu(PMe_3)_2]_2(\mu\text{-}S_2)$[12] 2.309(3) and 2.300(3) Å, $[(PhNCHS)Ru(CO)(PPh_3)]_2(MS_4)\cdot 2(CH_3)_2CO$[11] 2.359(3) (M = Mo) and 2.347(5) Å (M = W)).

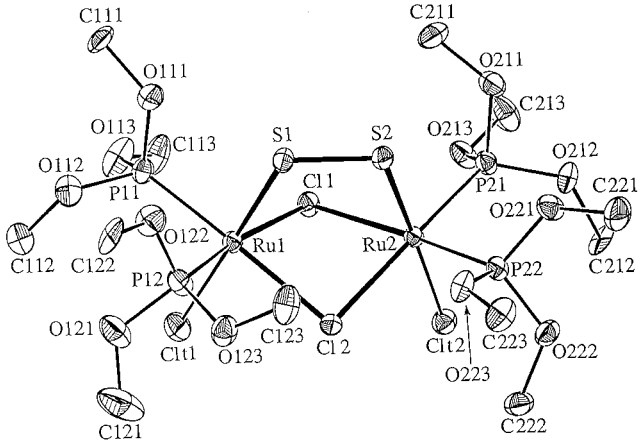

Figure 1. Structure of $[\{RuCl(P(OMe)_3)_2\}_2(\mu\text{-}Cl)_2(\mu\text{-}S_2)]$ **(1)**.

Table 2. Major Interatomic Distances (Å) for **1**, **2(CF$_3$SO$_3$)**, **3(PF$_6$)$_3$**, **4**, and **5**

	1		
Ru1−Ru2	3.579(1)	S1−S2	1.971(4)
Ru1−Cl1	2.530(2)	Ru2−Cl1	2.504(2)
Ru1−Cl2	2.484(3)	Ru2−Cl2	2.488(2)
Ru1−Clt1	2.420(2)	Ru2−Clt2	2.426(3)
Ru1−S1	2.205(2)	Ru2−S2	2.198(3)
Ru1−P11	2.248(3)	Ru2−P21	2.258(2)
Ru1−P21	2.242(3)	Ru2−P22	2.252(2)
	2(CF$_3$SO$_3$)		
Ru1−Ru2	3.536(2)	S1−S2	1.972(7)
Ru1−S1	2.191(5)	Ru2−S2	2.226(5)
Ru1−Cl1	2.473(5)	Ru2−Cl1	2.475(5)
Ru1−Cl2	2.498(5)	Ru2−Cl2	2.467(5)
Ru1−Cl3	2.401(5)	Ru2−P3	2.247(5)
Ru1−P1	2.256(5)	Ru2−P4	2.240(6)
Ru1−P2	2.249(6)	Ru2−N	2.076(17)
	3(PF$_6$)$_3$		
Ru1−S1	2.322(2)	Ru1−N1	2.127(7)
Ru1−P1	2.234(3)	Ru1−N2	2.154(9)
Ru1−P2	2.232(4)	Ru1−N3	2.054(7)
S1−S1′	1.995(3)		
	4		
Ru−S1	2.197(3)	Ru−P2	2.247(4)
Ru−Cl	2.483(3)	Ru−N1	2.08(1)
Ru−Cl′	2.478	S1−S1′	1.973(7)
Ru−P1	2.252(4)		
	5		
Ru1−S1	2.279(9)	Ru−S2	2.245(9)
Ru1-P1	2.304(9)	Ru2−P3	2.265(9)
Ru1−P2	2.273(9)	Ru2−P4	2.305(10)
Ru1−N1	2.20(3)	Ru2−N4	2.16(3)
Ru1−N2	2.12(3)	Ru2−N5	2.21(3)
Ru1−N3	2.10(2)	Ru2−N6	2.12(3)
S1−S2	1.933(11)		

(31) Heeres, H. J.; Meetsma, A.; Teuben, J. H. *Angew. Chem., Int. Ed. Engl.* **1990**, *29*, 420.
(32) Pregosin, P. S.; Roulet, R. F. R.; Michelin, T. B. R. A.; Ros, R. *Inorg. Chim. Acta* **1980**, *45*, L7.
(33) Mizobe, Y.; Hosomizu, M.; Kawabata, J.; Hidai, M. *J. Chem. Soc., Chem. Commun.* **1991**, 1226.
(34) Rauchfuss, T. B.; Rodgers, D. P. S.; Wilson, S. R. *J. Am. Chem. Soc.* **1986**, *108*, 3114.

Table 3. Interatomic Angles (deg) of the RuSSRu Cores in **1**, **2(CF$_3$SO)**, **3(PF$_6$)$_3$**, **4**, and **5**

	1		
Cl1−Ru1−Cl2	79.01(8)	Cl1−Ru2−Cl2	79.44(6)
Cl1−Ru1−S1	87.66(8)	Cl1−Ru2−S2	88.11(9)
Cl2−Ru1−S1	92.65(8)	Cl2−Ru2−S2	92.51(9)
Ru1−S1−S2	111.3(2)	Ru2−S2−S1	111.5(1)
Ru1−Cl1−Ru2	90.61(6)	Ru1−Cl2−Ru2	92.07(7)
	2(CF$_3$SO$_3$)		
Cl1−Ru1−Cl2	80.1(2)	Cl1−Ru2−Cl2	80.1(2)
Cl1−Ru1−S1	92.1(2)	Cl1−Ru2−S2	91.8(2)
Cl2−Ru1−S1	88.9(2)	Cl2−Ru2−S2	89.7(2)
Ru1−S1−S2	111.8(3)	Ru2−S2−S1	109.6(3)
Ru1−Cl1−Ru2	91.2(1)	Ru1−Cl2−Ru2	90.8(1)
	3(PF$_6$)$_3$		
Ru1−S1−S1′	107.5(1)		
	4		
Cl−Ru−S1	92.4(1)		
	5		
Ru1−S1−S2	108.6(4)	S1−S2−Ru2	109.9(5)

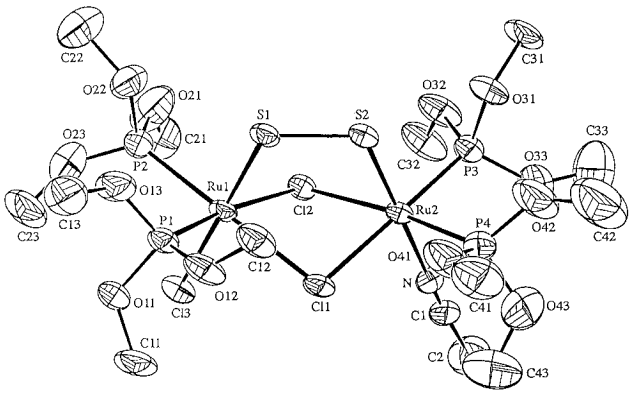

Figure 2. Structure of [{RuCl(P(OMe)$_3$)$_2$}$_2$(μ-Cl)$_2$(μ-S$_2$){Ru(CH$_3$CN)(P(OMe)$_3$)$_2$}]$^+$ (**[2]**$^+$).

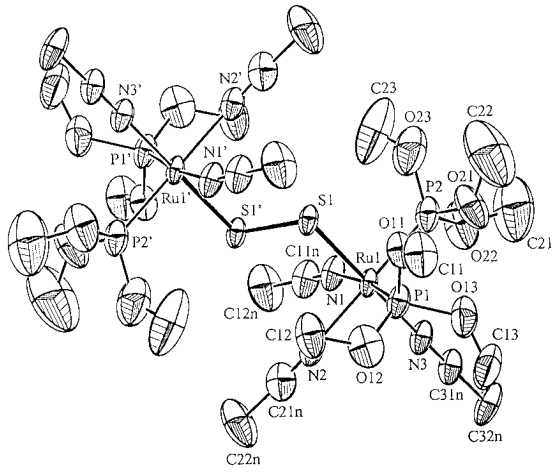

Figure 3. Structure of the major component of [{Ru(CH$_3$CN)$_3$(P(OMe)$_3$)$_2$}$_2$(μ-S$_2$)]$^{3+}$ (**[3]**$^{3+}$).

Structure of 2(CF$_3$SO$_3$). The structure of **[2]**$^+$ is shown in Figure 2. The complex cation has basically the same structure as **1**, except that one of the two terminal chlorides in **1** is replaced by CH$_3$CN in **2**. The major atomic distances and angles are listed in Tables 2 and 3, respectively. All the interatomic distances and angles are listed in Tables S18 and S19, respectively, in the supporting information. The Ru−Ru distance of 3.536(2) Å is significantly shorter than that of **1**. The Ru1−S1 distance of 2.191(5) Å is shorter than that of **1** and shows significant double-bond character, whereas Ru2−S2 of 2.226(5) Å is longer than Ru1−S1. The S−S distance of 1.972(7) Å is not much different from the corresponding one in **1**. The Ru−S−S angles of 111.8(3)° and 109.6(3)° (Table 3) are also the same as those of **1**.

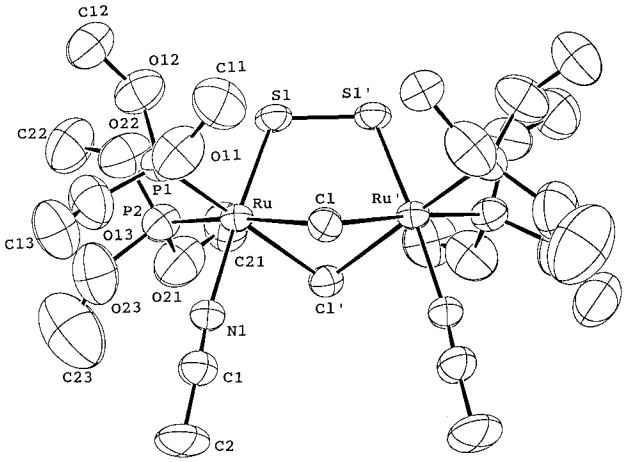

Figure 4. Structure of [{Ru(CH$_3$CN)(P(OMe)$_3$)$_2$}$_2$(μ-Cl)$_2$(μ-S$_2$)]$^{2+}$ (**[4]**$^{2+}$).

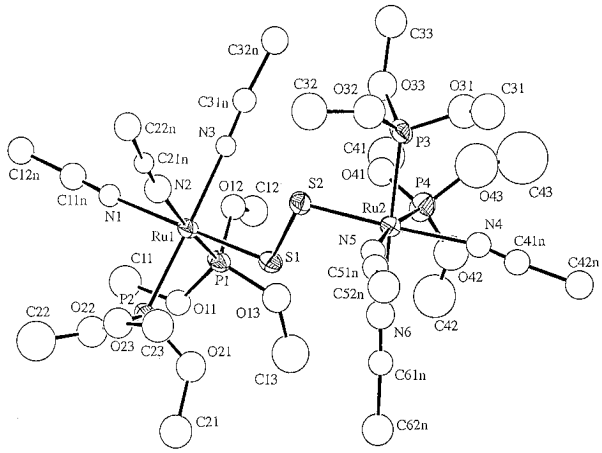

Figure 5. Structure of [{Ru(CH$_3$CN)$_3$(P(OMe)$_3$)$_2$}$_2$(μ-S$_2$)]$^{4+}$ (**[5]**$^{4+}$).

Structure of 3(PF$_6$)$_3$. The structure of the major component of the two disordered **[3]**$^{3+}$ complexes is shown in Figure 3. The structure of the minor component is shown in the Figure S2. The coordination distances and angles are listed in Tables 2 and 3. All the interatomic distances and angles are listed in Tables S20 and S21, respectively, in the supporting information. All the *trans*-RuSSRu cores previously reported[12,35−37] are Ru^{III}-SSRu^{III}, and **[3]**$^{3+}$ is the first example of a mixed-valent one-electron reduced Ru^{II}SSRu^{III} core, whose structure is elucidated by X-ray diffraction analysis. The S−S distance of **[3]**$^{3+}$ is comparable to those of other disulfide-bridged cis and trans dimers, whereas the Ru−S distance of 2.322(2) Å in **3** is significantly longer than those of other complexes in Table 4. This significant difference is due to the one-electron reduction of the RuSSRu core. The literature values indicate that Ru^{II}−S distances are generally longer than Ru^{III}−S distances, i.e., 2.464 (av) Å in [{Ru^{II}(P(OMe)$_3$)$_4$}$_2$(μ-WS$_4$)](PF$_6$)$_2$,[10] 2.393 (av) Å in [{Ru^{II}(PhNCHS)(CO)(PPh$_3$)}$_2$(μ-WS$_4$)],[11] and 2.433 (av) Å in [{Ru^{II}(bpy)$_2$}$_2$(μ-SPh)$_2$](F$_3$CSO$_3$)$_2$.[30] Unfortunately, there has never been a Ru^{II}SSRu^{II} compound synthesized, and therefore, the Ru^{II}−S(disulfide) distance is not available in the literature. The Ru−S distance in **[3]**$^{3+}$ seems approximately an average of Ru^{II}−S and Ru^{III}−S distances. The Ru−S1−S1′ angle of

(35) Brulet, C. R.; Isied, S. S.; Taube, H. *J. Am. Chem. Soc.* **1973**, *95*, 4758.
(36) Luginbuhl, W.; Zbinden, P.; Pittet, P. A.; Armbruster, T.; Burgi, H.; Merbach, A. E.; Ludi, A. *Inorg. Chem.* **1991**, *30*, 2350.
(37) Holzer, W.; Murphy, W. F.; Bernstein, H. J. *J. Mol. Spectrosc.* **1969**, *32*, 13.

Table 4. Structure and Spectroscopic Properties

	−S−S−type	Ru−S (Å)	S−S (Å)	RR[a] $\nu_{(Ru-S)}$ (cm^{-1})	RR[a] $\nu_{(S-S}$ (cm^{-1})	ESR	ref
[{RuCl(TMP)$_2$}$_2$(μ-Cl)$_2$(μ-S$_2$)	*cis*	2.202 (av)	1.971	385 (s)	456 (vw)	diamagnetic	this work
[{RuCl(TMP)$_2$}(μ-Cl)$_2$(μ-S$_2$)[{Ru(AN)-(TMP)$_2$}](PF$_6$)	*cis*	2.209 (av)[c]	1.972[c]	379 (m), 410 (m)	454 (w)	diamagnetic	this work
[{Ru(AN)$_3$(TMP)$_2$}(μ-S$_2$)](PF$_6$)$_3$	*trans*	2.322	1.995	*e*	561 (s)	$g_x = 2.11$, $g_y =$ 20.5, $g_z =$ 1.994	this work
[{Ru(AN)(TMP)$_2$}$_2$(μ-S$_2$)(μ-Cl)$_2$](CF$_3$SO$_3$)$_2$	*cis*	2.197	1.973			diamagnetic	this work
[{Ru(AN)$_3$(TMP)$_2$}$_2$(μ-S$_2$)](CF$_3$SO$_3$)$_4$	*trans*	2.262	1.933			diamagnetic	this work
[{CpRu(PMe$_3$)$_2$}$_2$(μ-S$_2$)](SbF$_6$)$_2$	*trans*	2.208	1.962				12
[{CpRu(PPh$_3$)$_2$}$_2$(μ-S$_2$)](BF$_4$)$_2$	*trans*			414 (s)	530 (w)		12
[{CpRu(PPh$_3$)$_2$}$_2$(μ-S$_2$)](SbF$_6$)	*trans*					$g = 2.05$, $A =$ 7.2 G, 5-lines	12
[{Ru(NH$_3$)$_5$}$_2$(μ-S$_2$)]Cl$_4$·2H$_2$O	*trans*	2.193 (av)	2.014	415 (s)	519 (vw)	diamagnetic	35−37
1,4-[{(MeCp)Ru(PPh$_3$)}$_2$(μ-S$_2$)$_2$]	*trans*	2.295 (av)	2.046			diamagnetic	13
[{Ru(PPh$_3$)'S$_4$'}$_2$(μ-S$_2$)]·CS$_2$[d]	*trans*	2.244 (av)	1.991	372 (*RR*/*SS*)[b] (s) 384 (*RS*)[b] (s)	536 (*RR*/*SS*)[b] (m) 525 (*RS*)[b] (m)	diamagnetic	16
[{(η^5-C$_5$Me$_5$)Ru}$_2$(μ-SPr^i)$_2$(μ-S$_2$)]	*cis*	2.212 (av)	2.008			diamagnetic	33
[(μ_2-S$_2$){(η^5-C$_5$Me$_5$)Ru}$_2$(μ_3-S)$_2$(μ_2-S)$_2$WS]	*cis*	2.220 (av)	1.991				33
[{(η^5-C$_5$Me$_4$Et)Ru}$_2$(μ,η^2-S$_2$)(μ,η^1-S$_2$)]	*cis*	2.195	2.020				34

[a] Resonance Raman. [b] Isomers, see ref 16. [c] The bond distances are those of the $CF_3SO_3^-$ salt. [d] 'S$_4$' = 1,2-bis[(2-mercaptophenyl)thio]ethane-(2−), TMP = P(OMe)$_3$, AN = CH$_3$CN. [e] Not observed.

107.5(1)° is slightly smaller than those of the other trans dimer compounds listed in Table 4; the angles of the Ru−S−S groups in the compounds range from 110.1° to 113.9°. The angle Ru1−N3−C31 trans to the disulfide bridge is 176(1)°, which is comparable to those found in [Ru(η^6-C$_6$H$_6$)(CH$_3$CN)$_3$](PF$_6$)$_2$[36] (175.6(av)°). The angles cis to the disulfide are Ru1−N1−C11 = 162(1)° and Ru1−N2−C21 = 165(1)° and are obviously smaller than those trans to the disulfide. The large bend in the CH$_3$CN coordination in the cis position seems to be caused by the steric bulkiness of the P(OMe)$_3$ ligands cis to the CH$_3$CN ligands.

Structure of 4. The structure of **4** is shown in Figure 4. The major bond distances and angles are listed in Tables 2 and 3, while all the bond distances and angles are tabulated in Tables S22 and S23, respectively, in the supporting information. No significant difference is observed in the Ru−S and S−S distances of the three compounds having a Ru$_2$(μ-S$_2$)(μ-Cl)$_2$ core, **1**, **2**, and **4**, as Table 4 shows.

Structure of 5. The structure of **5** is shown in Figure 5. The major bond distances and angles are listed in Tables 2 and 3, whereas all the bond distances and angles are tabulated in Tables S24 and S25, respectively, in the supporting information. The bridged core structures of **[3]**$^{3+}$ and **[5]**$^{4+}$ are compared in Figure S3. The Ru−S distance in the Ru^{II}SSRu^{III} core of **[3]**$^{3+}$ is longer than those in the Ru^{III}SSRu^{III} core of **[5]**$^{4+}$. The S−S distance in Ru^{II}SSRu^{III} is also longer than that in Ru^{III}SSRu^{III}. The elongation in the reduced core is consistent with the π-MO description of the RuSSRu core, as detailed in the next section. The one additional electron of Ru^{II}SSRu^{III} enters an antibonding MO, thus lengthening the bond distances. The Ru−S−S−Ru torsion angles are 180.0° in **[3]**$^{3+}$ and 168.0(3)° in **[5]**$^{4+}$.

UV−Vis and Resonance Raman Spectra. The UV−vis spectra of compounds **1**, **2(PF$_6$)**, and **3(PF$_6$)$_3$** are shown in Figure 6. Those of **4** and **5** are shown in Figure 7. None of the compounds have any near-IR absorptions up to 2000 nm. Although the spectrum of **5** was measured in a N$_2$ atmosphere, it gradually degraded with an absorption decrease at λ_{max} of 652 nm, and the final spectrum was the same as that of **3**. Therefore, the spectral change in Figure 7 corresponds to the reduction of **[5]**$^{4+}$ to **[3]**$^{3+}$ by CH$_3$CN. The resonance Raman spectra of **1**, **2(PF$_6$)**, and **3(PF$_6$)$_3$** are shown in Figures 8, 9, and 10, respectively. Compound **1** shows a strong absorption band at 737 nm and exhibits resonance Raman bands at 385 cm^{-1} (ν(Ru−S), strong), 456 cm^{-1} (ν(S−S), very weak), and 769 cm^{-1} (double harmonics of 385 cm^{-1}). The assignment

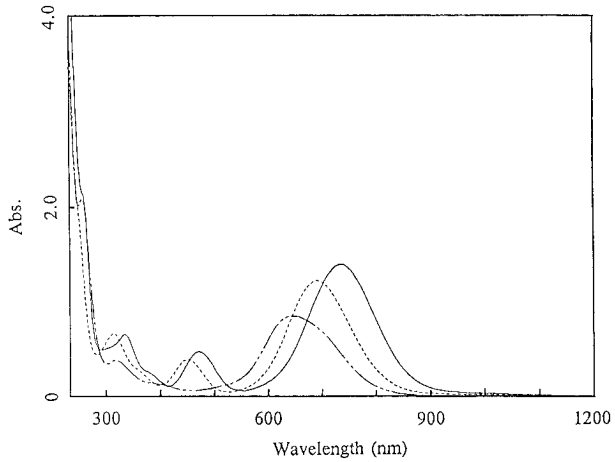

Figure 6. UV−vis spectra of **1** (—, 1.44 × 10^{-4} M), **2(PF$_6$)** (- - -, 1.40 × 10^{-4} M), and **3(PF$_6$)$_3$** (— - - —, 1.33 × 10^{-4} M) in CH$_3$CN.

was made on the basis of the reported values of analogous compounds.[8,10,11,16,37] The 385 cm^{-1} (ν(Ru−S)) and 456 cm^{-1} (ν(S−S)) bands of **1** should be compared (Table 4) to the reported values: 384 and 372 cm^{-1} (ν(Ru−S)) and 536 and 525 cm^{-1} (ν(S−S)) in the two isomers of [{μ-S$_2$){Ru^{III}-(PPh$_3$)'S$_4$'}$_2$], where 'S$_4$' is 1,2-bis[(2-mercaptophenyl)thio]-ethane(2−),[16] 415 cm^{-1} (ν(Ru−S)) and 519 cm^{-1} (ν(S−S)) in [{Ru^{III}(NH$_3$)$_5$}$_2$(μ-S$_2$)]Br$_4$,[15] and 409 (ν(Ru−S)) and 530 cm^{-1} (ν(S−S)) in [{CpRu^{III}(PPh$_3$)$_2$}$_2$(μ-S$_2$)](BF$_4$)$_2$.[12] These compounds are the only three *trans*-Ru^{III}SSRu^{III} ones for which UV−vis and resonance Raman spectra are reported; no Raman spectral data are available for *cis*-RuSSRu compounds other than **1** and **2**. The ν(S−S) frequencies in disulfide complexes generally range from 480 to 600 cm^{-1},[8] which should be compared to free S$_2$ (725 cm^{-1}),[38] S$_2^-$ (589 cm^{-1}),[37,39] and S$_2^{2-}$ (446 cm^{-1}).[8] The emission band of **1** at 385 cm^{-1} is more strongly enhanced by 647.1 nm radiation than by 568.2 nm. Therefore, the UV−vis absorption at 737 nm is considered to be the electronic transition within the Ru$_2$S$_2$ core. Compound **2(PF$_6$)** exhibits a strong visible absorption band at 690 nm. The resonance Raman spectrum of **2(PF$_6$)** shows emission bands at 379 and 410 cm^{-1}, which are assigned to ν(Ru−S). The 379 cm^{-1} band is only slightly shifted compared to the corresponding band in **1** and is therefore assigned to ν(Ru−S) of the ruthenium

(38) Bunker, B. C.; Drago, R. S.; Hendrickson, D. N.; Richman, R. M.; Kessell, S. L. *J. Am. Chem. Soc.* **1978**, *100*, 3805.
(39) Clark, R. J. H.; Cobbold, D. G. *Inorg. Chem.* **1978**, *17*, 3169.

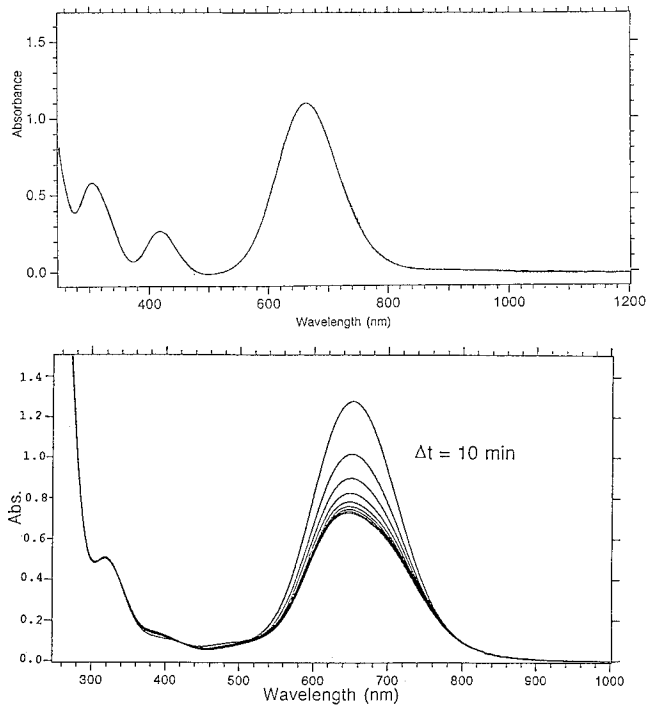

Figure 7. UV−vis spectra of **4** (upper, 1.47×10^{-4} M) and **5** (lower, 1.81×10^{-4} M) in CH_3CN.

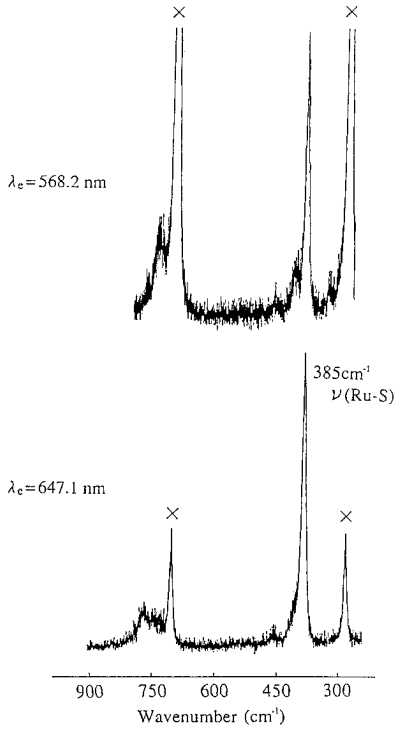

Figure 8. Resonance Raman spectra of **1** in CH_2Cl_2 (4.42×10^{-3} M). λ_e is the excitation wavelength. X: CH_2Cl_2.

atom with the terminal chloride, whereas the 410 cm^{-1} band is assigned to ν(Ru−S) of the Ru atom with the terminal CH_3-CN. These two bands are more strongly enhanced by λ_e = 647.1 nm than by λ_e = 476.5 and 568.2 nm, and therefore the UV−vis band at 689 nm can be assigned to the transition of the Ru_2S_2 core. The very weak band of **2(PF$_6$)** at 454 cm^{-1} is ν(S−S) as judged by analogy to the corresponding weak band of **1** at 456 cm^{-1}. Compound **3(PF$_6$)$_3$** exhibits strong visible absorption at 646 nm, which is analogously assigned to the transition within the Ru_2S_2 core. The resonance Raman spectrum of **3(PF$_6$)$_3$** shows a strong ν(S−S) band at 561 cm^{-1}, which is stronger with λ_e = 647.1 than λ_e = 568.2 nm. The

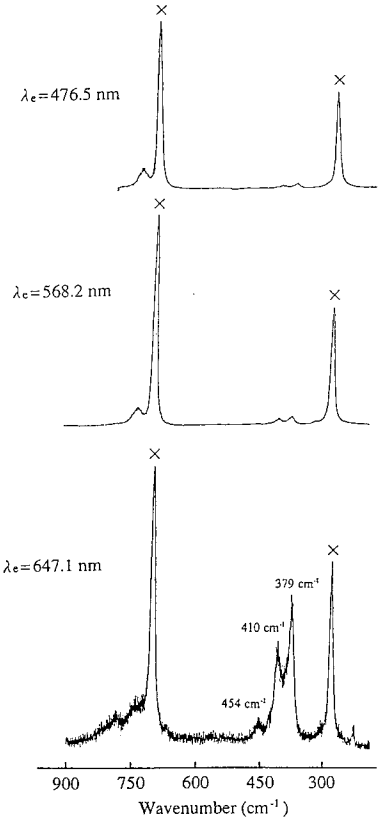

Figure 9. Resonance Raman spectra of **2(PF$_6$)** in CH_2Cl_2 (9.02×10^{-4} M). λ_e is the excitation wavelength. X: CH_2Cl_2.

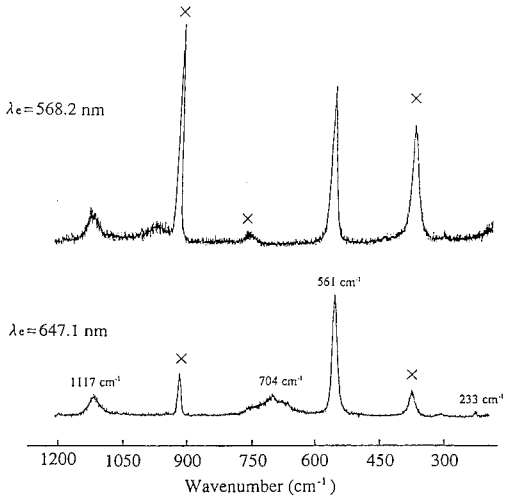

Figure 10. Resonance Raman spectra of **3(PF$_6$)$_3$** in CH_3CN (9.56×10^{-4} M). λ_e is the excitation wavelength. X: CH_3CN.

band of ν(Ru−S) could not be observed for **3(PF$_6$)$_3$** in CH_3-CN, while a strong ν(S−S) band was observed at 561 cm^{-1}. The ν(Ru−S) band would be in the range 370−400 cm^{-1}, which is, however, obscured by the Raman band of the solvent. Even if the ν(Ru−S) band exists in the area, the intensity must be very weak. Acetonitrile has to be used as the solvent, in order to avoid the release of the coordinated CH_3CN.

It should be noted that for complexes with a *cis*-RuSSRu core, **1** and **2**, ν(Ru−S) is strongly enhanced, whereas ν(S−S) is only very weakly observed. This is in remarkable contrast with complex **[3]**$^{3+}$ with a *trans*-RuSSRu core, which exhibits only a strong ν(S−S) in CH_3CN; ν(Ru−S) is very weak or is not enhanced. The resonance Raman spectrum of $[(H_3N)_5RuSSRu(NH_3)_5]^{4+}$ with a planar *trans*-$Ru^{III}SSRu^{III}$ core[15] exhibits strong ν(Ru−S) but no ν(S−S), when excited by 647.1 nm. This excitation wavelength is close to the visible absorption maxi-

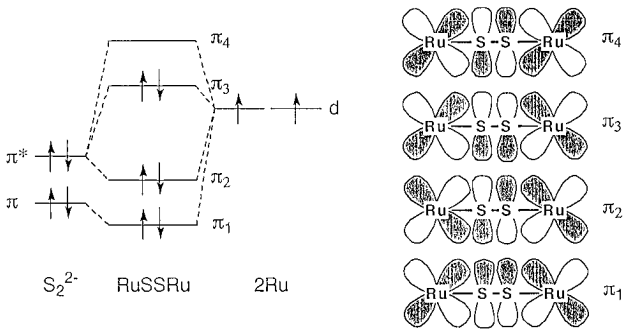

Figure 11. π-MO scheme for a $Ru^{III}SSRu^{III}$ core.

mum of the complex at 715 nm. The ν(S−S) at 514 cm^{-1} is observed only when it is excited by shorter wavelengths, i.e., by 568.2 nm or less.[15] The resonance Raman and electronic bands can be reasonably explained by a qualitative MO description of the RuSSRu core as follows. The electronic transitions in the visible region correspond to a LMCT (ligand to metal charge transfer) from S_2^{2-} to Ru(III). A resonance Raman band with significant magnitude should be observable only for symmetric ν(Ru−S) when the solution is irradiated by the visible band. The theory also predicts that the intensity of the ν(S−S) band is zero.[15] A basically similar but simpler explanation can be given to the electronic absorption bands of $[\{Ru(PPh_3)'S_4'\}_2(\mu\text{-}S_2)]\cdot CS_2$.[16] In order to obtain a clear image of the electronic states and to explain the Raman and ESR spectra (see later section) of the present compounds, the π-MO scheme for a RuSSRu core is given in Figure 11, which is basically similar to what is described in ref 16. The strong visible absorptions of compounds **1**, **2(PF$_6$)**, **3(PF$_6$)$_3$**, **4**, and **5** are the transitions from π_3 to π_4, which is LMCT. This assignment has been confirmed by the fact that a hypsochromic shift is observed for the visible absorption bands when Lewis acid is added to the solution. For instance, the λ_{max} of **1** at 734 nm in CH_2Cl_2 shifts to 697 nm when 1 equiv of $SnCl_4$ is added to the solution. The compounds **1**, **2**, **4**, and **5** are diamagnetic, since the two unpaired electrons of the two low-spin Ru(III) ions are paired as shown in Figure 11. Compound **[3]**$^{3+}$ with a $Ru^{II}SSRu^{III}$ core is paramagnetic, since its one unpaired electron is in the π_4 orbital. Among the eight compounds with a *trans*-$Ru^{III}SSRu^{III}$ core so far reported (Table 4), only $[\{Ru(PPh_3)'S_4'\}_2(\mu\text{-}S_2)]\cdot CS_2$ exhibits the $\pi_3-\pi_4$ band near 1000 nm, whereas all the others are at around 700 nm. It is noteworthy that, for the three compounds with a *trans*-$Ru^{III}SSRu^{III}$ core, $[\{CpRu(PPh_3)_2\}_2(\mu\text{-}S_2)](BF_4)_2$, $[\{Ru(NH_3)_5\}_2(\mu\text{-}S_2)]Cl_4\cdot 2H_2O$, and $[\{Ru(PPh_3)'S_4'\}_2(\mu\text{-}S_2)]\cdot CS_2$, the ν(S−S) Raman bands are very weak and the ν(Ru−S) are strong (Table 4). This relative intensity relation is completely reversed in compound **3(PF$_6$)$_3$** having a *trans*-$Ru^{II}SSRu^{III}$ core. Only a strong ν(S−S) band is observed for **[3]**$^{3+}$. Kim et al. explains that the strong ν(Ru−S) band in *trans*-$Ru^{III}SSRu^{III}$ is aroused by a transition associated with a symmetric Ru−S stretch, and thus only the ν(Ru−S) band is enhanced by the visible band to a significant intensity;[15] the stretching of the S−S bond does not contribute to the dipole moment responsible for the visible electronic absorption. If, however, the core is reduced to *trans*-$Ru^{II}SSRu^{III}$, a dipole moment, raised by the electronic transition between the mixed-valent two metals, would operate along the S−S bond.[15] In addition, the compound would experience less LMCT, since the metal is reduced by one electron. Both of these factors would in effect enhance the ν(S−S) strongly and weaken the ν(Ru−S). The relative intensity of ν(S−S) to ν(Ru−S) is large for $[\{Ru(PPh_3)'S_4'\}_2(\mu\text{-}S_2)]\cdot CS_2$, compared to that of $[(NH_3)_5RuSSRu(NH_3)_5]^{4+}$ (Table 4), since the *trans*-RuSSRu core of the former complex deviates largely from a planar structure, caused by steric demands of the 'S_4' and PPh_3 ligands. The latter complex has a planar *trans*-RuSSRu core in X-ray crystal structure.[14] Although the frequencies of ν(S−S) for **1** and **2** (456 and 454 cm^{-1}, respectively) are considerably lower than those of the trans cores (Table 4), the additional Cl^- bridges in **1** and **2** might have caused significant differences in the electronic structures of the cores, lowering the ν(S−S) frequencies. Although comparison of the Raman spectra of **[3]**$^{3+}$ and **[5]**$^{4+}$ is valuable, a reliable spectrum of **[5]**$^{4+}$ is valuable, a reliable spectrum of **[5]**$^{4+}$ could not be obtained, since the compound is too unstable even in a N_2 atmosphere.

^{31}P{^{1}H} NMR Spectrum. The ^{31}P{^{1}H} NMR spectrum of **2(PF$_6$)** in CD_3CN exhibits two singlets at 124.3 and 114.5 ppm with almost equal intensities. Compound **2(CF$_3$SO$_3$)** exhibits peaks at 125.3 and 115.6 ppm in CD_3CN. The former signals of both compounds are ascribed to $P(OMe)_3$ coordinated to the Ru atom with a terminal chloride, since the chemical shift is only slightly shifted from that of **1** (123.8 ppm in CD_3CN). The signal at 114.5 ppm of **2(PF$_6$)** is accordingly ascribed to the $P(OMe)_3$ coordinated to the other Ru atom. The ^{31}P signal of **3(PF$_6$)$_3$** and **3(CF$_3$SO$_3$)$_3$** could not be observed except for that of PF_6^- at −145.6 ppm, which is probably due to the paramagnetism of the complex cation. The ^{31}P{^{1}H} signal of **4** is a broad singlet at 117 ppm with $\nu_{1/2}$ = 360 Hz in CD_3CN. The reason for such unusual broadening is not known. The signal was compared to that of **1** in CD_3CN with the addition of 2 equiv of $AgCF_3SO_3$ (Figure S4). The latter solution should contain **4**, and the UV−vis spectrum is actually identical to that of **4** (λ_{max} = 664 nm). However the ^{31}P resonance peak is not broadened, having an identical chemical shift at 117.3 ppm.

ESR Spectra of 3(PF$_6$)$_3$. Complex **[3]**$^{3+}$ is the first well-characterized mixed-valent complex with a *trans*-$Ru^{II}SSRu^{III}$ core, which is ESR active due to the Ru(III) atom. All other $Ru^{III}SSRu^{III}$ complexes in the present study and those so far reported are diamagnetic. Therefore, the ESR spectrum of **[3]**$^{3+}$ is valuable for elucidating the intervalence interaction occurring between the two Ru atoms through the distinct S_2^{2-} ligand.

The powder and solution ESR spectra of **3(PF$_6$)$_3$** are shown in Figure 12. The powder spectrum at 288 K shows a rhombic signal of the unpaired electron of Ru(III) with g_1 = 2.12, g_2 = 2.05, and g_3 = 1.995. Although several ESR spectra of mononuclear and dinuclear paramagnetic Ru(III) complexes have been analyzed with the matrix of a spin−orbit coupling Hamiltonian, most of them have axial symmetry with only $g_\perp$ and $g_\parallel$ parameters.[38] Rhombic spectral analysis of g_x, g_y, and g_z, by using spin−orbit coupling constant λ, axial splitting parameter Δ, and rhombic splitting parameter V, is reported only for monomeric Ru(III) complexes[29] with phosphine and other nitrogen-donor ligands. The rhombic anisotropy in Figure 12 is remarkably small, compared to those of the reported monomeric and dimeric Ru(III) complexes with axial or rhombic symmetries.[39,40] Low-spin Ru(III) species exhibit ESR spectra which are usually highly anisotropic with axial or rhombic symmetry.[29,41] For example, $[Ru^{III}(NH_3)_4(cat)]^+$ (cat is catecholate and its derivatives) cations give axial spectra with $g_\parallel$ = ∼1.9 and $g_\perp$ = ∼2.7.[42] However, in certain reduced $[Ru(bpy)_3]^{(2-n)+}$ species, the unpaired electron is delocalized over the metal and the ligand, and shows only a slightly anisotropic signal with g-value differences of up to ∼0.04.[43] In

(40) Cotton, F. A.; Torralba, R. C. *Inorg. Chem.* **1991**, *30*, 4392.
(41) (a) Desimone, R. E. *J. Am. Chem. Soc.* **1973**, *95*, 6238. (b) Sakaki, S.; Hagiwara, N.; Yanase, Y.; Ohyoshi, A. *J. Phys. Chem.* **1978**, *82*, 1917. (c) Raynor, J. B.; Jeliazkowa, B. G. *J. Chem. Soc., Dalton Trans.* **1982**, 1185.
(42) Pell, S. D.; Salmonsen, R. B.; Abelleira, A.; Clarke, M. J. *Inorg. Chem.* **1984**, *23*, 385.
(43) (a) Motten, A. G.; Hanck, K. W.; DeArmond, M. K. *Chem. Phys. Lett.* **1981**, *79*, 541. (b) Morris, D. E.; Hanck, K. W.; DeArmond, M. K. *J. Am. Chem. Soc.* **1983**, *105*, 3032.

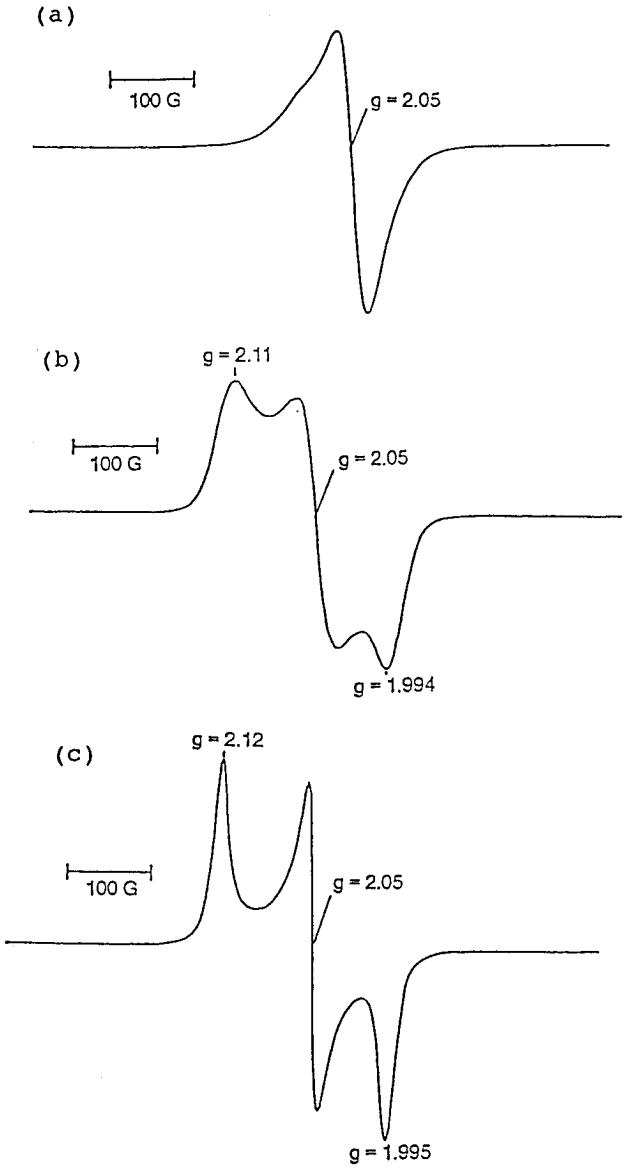

Figure 12. ESR spectra of $[\{Ru(CH_3CN)_3(P(OMe)_3)_2\}_2(\mu\text{-}S_2)](PF_6)_3$ **(3(PF$_6$)$_3$)**: (a) frozen CH_3CN solution at 223 K; (b) frozen CH_3CN solution at 188 K; (c) powder at 288 K.

semiquinone- and dioxolene-bridged dimeric Ru(III) complexes, very small anisotropy similar to **3** is known, in which the unpaired electron is substantially delocalized onto the bridging ligand.[44−46] The anisotropy is large and similar to those of usual monomeric low-spin Ru(III) species, when the electron delocalization onto the bridging ligand is a minimum, i.e., in the organoborane-bridged $Ru^{II}Ru^{III}$ dimer complex, an axial spectrum of significant anisotropy with a $g_\perp$ and $g_\parallel$ difference of ~0.3 is observed.[47]

The powder spectral pattern in Figure 12 was analyzed according to the matrix calculation described in the Experimental Section. The final best fit was obtained when $\lambda = 100$ cm^{-1}, $V = 1680$ cm^{-1}, $\Delta = -2690$ cm^{-1}, $k = 0.92$, and the corresponding calculated g values were $g_x = 2.109997$, $g_y = 2.049969$, and $g_z = 1.993901$. These g values are in excellent agreement with the experimental values in Figure 12. The best-fit λ value of 100 cm^{-1} is extraordinarily low, compared to the previously reported values for monomeric Ru(III) complexes; λ values are 884 cm^{-1} for $RuCl_3(P(n\text{-}Bu)_2Ph)_3$,[29a] 1007 cm^{-1} for $[Ru(H_2O)_6]^{3+}$,[48] and 1150 cm^{-1} for $[Ru(NH_3)_6]^{3+}$.[48] More generally, λ values of 700−1000 cm^{-1} are reported for low-spin Ru(III) complexes.[49] The low λ value of the present complex is, however, not extraordinary, since the extensive electron delocalization on the metal−ligand bond results in the transfer of some of the unpaired electron density onto the ligand. As a result, the orbital angular momentum is decreased, i.e., the orbital contribution is reduced, and thus the magnetic parameters become closer to the spin-only value of $g = 2$[49] as observed in the present complex **3(PF$_6$)$_3$**. The orbital reduction factor k of 0.92 is normal, compared to the literature values: 0.865 for $[Ru(H_2O)_6]^{3+}$,[48] 0.959 for $[Ru(NH_3)_6]^{3+}$,[48] 0.932 for $[Ru(bipy)_3](PF_6)_3$ (bipy is 2,2′-bipyridyl),[50] 0.912 for $[Ru(phen)_3](PF_6)_3$ (phen is phenanthroline),[50] 0.95 for $RuCl_3(PMe_2Ph)_3$,[29a] and 0.99 for $RuCl_3(AsPr_3)_3$.[29a] The reduced spin−orbital interaction in **[3]**$^{3+}$ does not contradict the π-MO scheme in Figure 11, since the distinct π-MO, composed of the π-orbitals of two Ru and two S atoms, corresponds to a delocalized electronic state between the metal and the sulfur atoms. The lack of near-IR absorption of **[3]**$^{3+}$ is not inconsistent with the π-MO scheme but suggests that the electronic state of **[3]**$^{3+}$ is actually beyond what the ligand field theory covers, and a MO treatment is a more realistic way to deal with the compound. The ESR spectrum of **[3]**$^{3+}$ with such small anisotropy is not common to Ru(III) complexes and means that the parameters, Δ and V, are small. Actually, the result of the present calculation shows relatively small splitting parameters, which should be compared to larger values of $\Delta = 5600$ cm^{-1} and $V = 2500$ cm^{-1} for the tris 8-quinolinol complex[29b] and $V = 5950$ cm^{-1} for $RuCl_3(P(n\text{-}Bu)_2Ph)_3$.[29a]

Electrochemistry. The cyclic voltammograms of **1**, **2(PF$_6$)**, and **3(PF$_6$)$_3$** are shown in Figure 13, together with that of the starting compound *trans*-$RuCl_2(P(OMe)_3)_4$. Compound **1** exhibits a quasi-reversible wave at −0.20 V (vs Ag/AgCl), which corresponds to a one-electron Ru(II/III) reaction. The potential is about 0.61 V cathodically shifted, compared to the Ru(II/III) potential of 0.41 V for the starting compound *trans*-$RuCl_2(P(OMe)_3)_4$. A similarly large cathodic shift has also been reported for disulfide-bridged compound $[\{CpRu(PPh_3)_2\}_2(\mu\text{-}S_2)](SbF_6)_2$,[12] whose one-electron Ru(II/III) redox wave is cathodically shifted by 1.45 V upon replacing the chloride ligand of the starting compound $CpRu(PPh_3)_2Cl$ with a disulfide bridging ligand. These facts show a strong π-donation of the disulfide ligand.[12] The Ru(II/III) wave of **2** is observed at +0.08 V (vs Ag/AgCl), which is anodically shifted from the corresponding wave of **1**. This is caused by the decrease of electron density at the ruthenium center in **2** by the substitution of the chloride in **1** to CH_3CN. Compound **3(PF$_6$)$_3$** exhibits a Ru(II,III)/Ru(II,II) irreversible wave at −0.30 V (vs Ag/AgCl) and quasi-reversible Ru(III,III)/Ru(II,III) wave at +0.74 V. The latter potential is significantly shifted anodically from those of **1** and **2**. It seems that an unknown electrocatalytic reaction occurs at both ends of the potential scans for **1**, **2**, and **3(PF$_6$)$_3$**, but the reactions were not examined in detail. The cyclic voltammogram of **5** could not be obtained, since the compound is too unstable.

X-ray Photoelectron Spectra of 1, 3(PF$_6$)$_3$, and 4. In XPS measurement, inadequate sample preparation, unsuitable mounting procedures, and X-ray irradiation damage of the sample can

(44) (a) Ernst, S.; Hänel, P.; Jordanov, J.; Kaim, W.; Kasack, V.; Roth, E. *J. Am. Chem. Soc.* **1989**, *111*, 1733. (b) Ernst, S.; Kasack, V.; Bessenbacher, C.; Kaim, W. *Z. Naturforsch.* **1987**, *42B*, 425.
(45) Masui, H.; Lever, A. B. P.; Auburn, P. R. *Inorg. Chem.* **1991**, *30*, 2402.
(46) Auburn, P. R.; Dodsworth, E. S.; Haga, M.; Liu, W.; Nevin, W. A. *Inorg. Chem.* **1991**, *30*, 3502.
(47) Merkert, J. W.; Davis, J. H., Jr.; Geiger, W. E.; Grimes, R. N. *J. Am. Chem. Soc.* **1992**, *114*, 9846.
(48) Daul, C.; Goursot, A. *Inorg. Chem.* **1985**, *24*, 3554.
(49) Goodman, B. A.; Raynor, J. B. *Adv. Inorg. Chem. Radiochem.* **1970**, *13*, 136.
(50) DeSimone, R. E.; Drago, R. S. *J. Am. Chem. Soc.* **1970**, *92*, 2343.

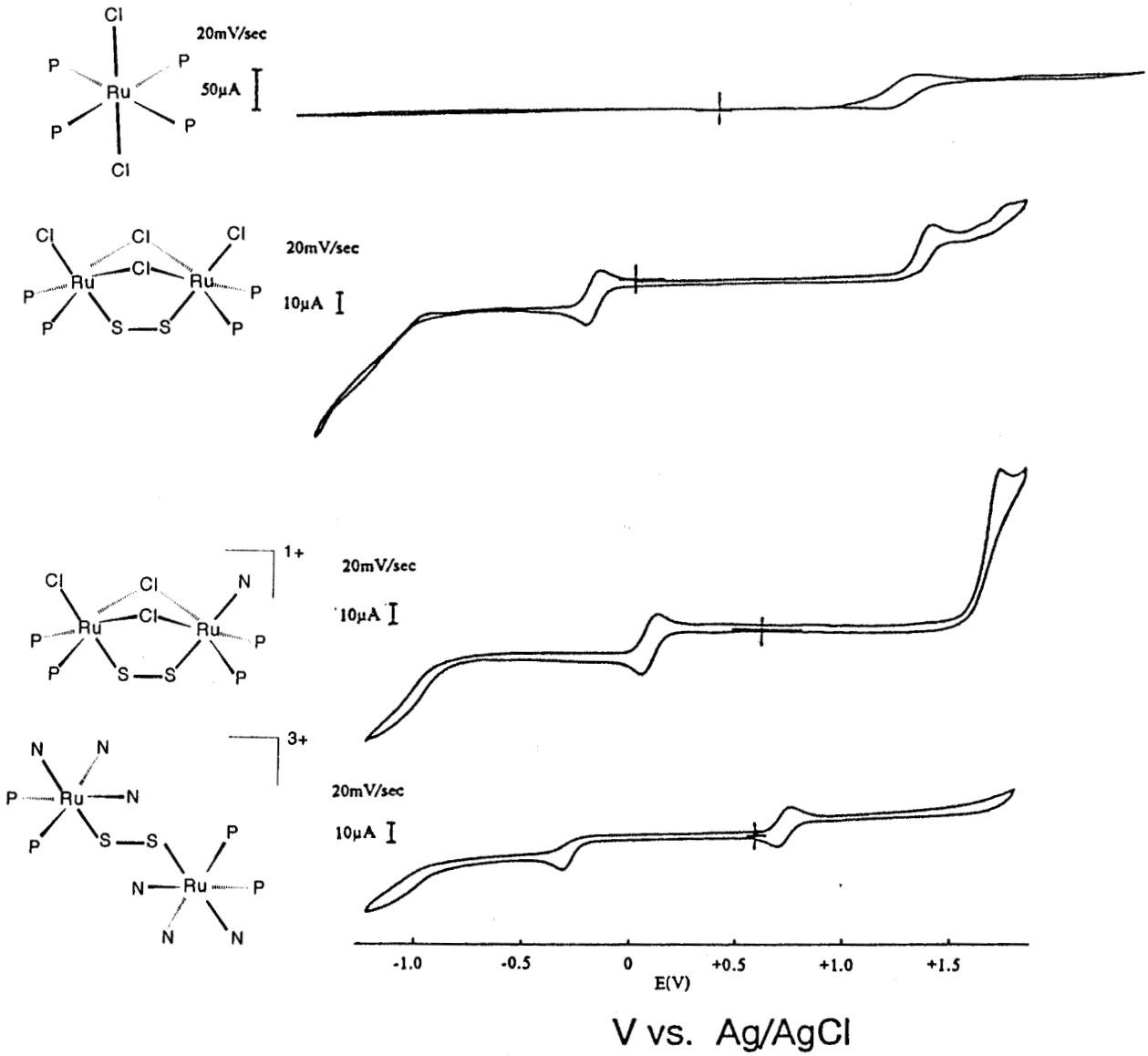

Figure 13. Cyclic voltammograms of **1**, **2(PF$_6$)**, **3(PF$_6$)$_3$**, and the starting compound *trans*-$RuCl_2(P(OMe)_3)_4$ in CH_3CN: 0.1 M TBAP as electrolyte; a Pt electrode; scan rate 20 mV/s. In the figure, P is $P(OMe)_3$, and N is CH_3CN.

sometimes cause undesired spectral deterioration and obscure the real spectral features.[51] In order to estimate and avoid these undesired effects, powder-dispersed In films were prepared in duplicate for each compound, and each film was measured twice. Compounds **1**, **3(PF$_6$)$_3$**, and **4** did not show significant spectral change on such repetitive sample preparations and measurements, whereas **5** received appreciable spectral change. Compound **5** is therefore not reported here.

Ru $3d_{5/2}$ and $3d_{3/2}$ spectra are shown in Figure 14. The binding energies are listed in Table 5. For each compound, the Ru $3d_{3/2}$ peak could not be clearly observed, because the C 1s peak of $P(OMe)_3$ overlaps on the Ru $3d_{3/2}$ peak. The binding energies of Ru $3d_{5/2}$ are summarized in Table 4, together with the binding energies of other elements. Contrary to our expectations, the Ru $3d_{5/2}$ binding energies do not show significant differences among the three compounds. Compound **3(PF$_6$)$_3$** is mixed-valent and as such had been expected to exhibit Ru(II) and Ru(III) components in the spectra. However, it actually shows only one component for each Ru $3d_{5/2}$ and $2P_{3/2}$, with the binding energies nearly equal to those of the Ru(III) dimer complexes **1** and **4**. The peak profiles of **3(PF$_6$)$_3$** are also similar to those of **1** and **2**, which rules out the possibility that two components of Ru(II) and Ru(III) are overlapped to be a broadened peak. The Ru $3d_{5/2}$ binding energies of the compounds are considerably closer to the literature values for Ru(II) than for Ru(III): Ru(III) $3d_{5/2}$ energies are 281.8−281.9 eV for $[Ru(X\text{-}Py)_2(DTBD_{iox})_2]ClO_4$ (X-Py is halogenated pyridine, and $DTBD_{iox}$ is a derivative of 1,2-dioxolene),[52] 282.1−282.3 eV for $[Ru(NH_3)_5L]^{3+}$ (L is various nitrogen donor ligands),[53] and 281.8 eV for $RuCl_3$.[54] The binding energies for Ru(II) are 279.5−281.8 eV for $[Ru(NH_3)_5L]^{2+}$,[53] 280.8−281.0 eV for $[Ru(X\text{-}Py)_2(DTBD_{iox})_2]$,[52] and 279.6−280.8 eV for [(η^5-CP*)Ru(η^5-Cp′)] (Cp* is pentamethylcyclopentadienyl and Cp′ is cyclopentadienyl derivatives).[55] The Ru $3P_{3/2}$ binding energies of the three compounds do not show any significant difference among themselves as well, and the values are close to those of Ru(II); Ru(II) $3P_{3/2}$ energies are 461.0−461.6 eV, whereas Ru(III) energies are 463.6−464.8 eV in the Creutz−Taube mixed-valent complexes of various counteranions.[51] The calibration of the binding energy by using the C 1s binding energy of the coordinated $P(OMe)_3$ in the compound does not

(51) Citrin, P. H.; Ginsberg, A. P. *J. Am. Chem. Soc.* **1981**, *103*, 3673.

(52) Auburn, P. R.; Dodsworth, E. S.; Haga, M.; Liu, W.; Nevin, A.; Lever, A. B. P. *Inorg. Chem.* **1991**, *30*, 3502.

(53) Shephered, R. E.; Proctor, A.; Henderson, W. W.; Myser, T. K. *Inorg. Chem.* **1987**, *26*, 2440.

(54) Moulder, J. F.; Stickle, W. F.; Sobol, P. E.; Bomben, K. D. *Handbook of X-ray Photoelectron Spectroscopy* Perkin-Elmer Co.: Edin Prairie, MN, 1992; p 115.

(55) Gassman, P. G.; Winter, C. H. *J. Am. Chem. Soc.* **1988**, *110*, 6130.

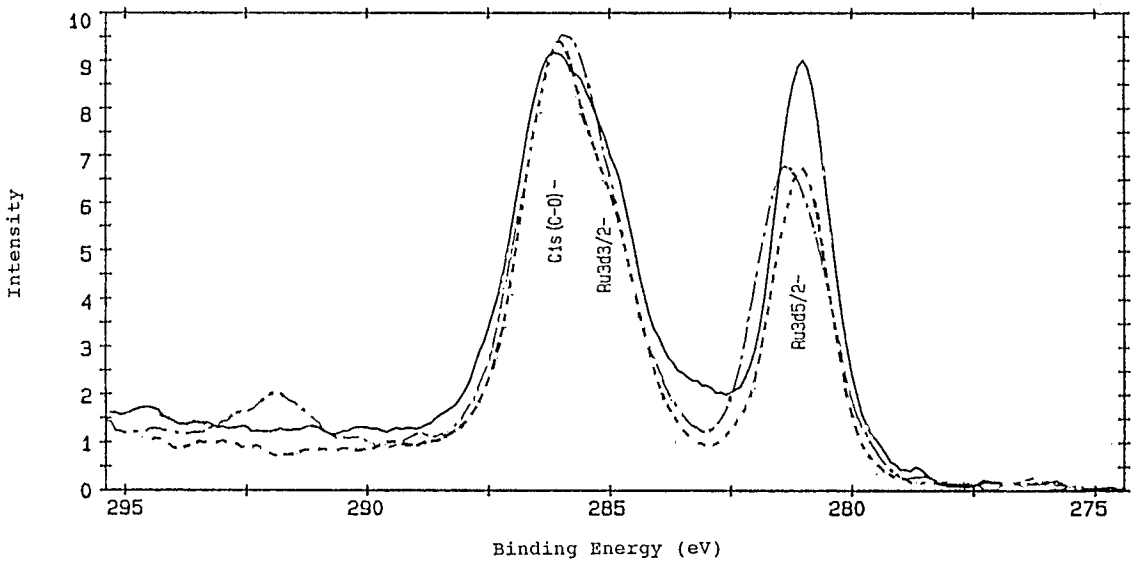

Figure 14. Ru $3d_{5/2}$, $3d_{3/2}$, and C 1s peaks of **1** (—), **3(PF$_6$)$_3$** (- - -), and **4** (— - —).

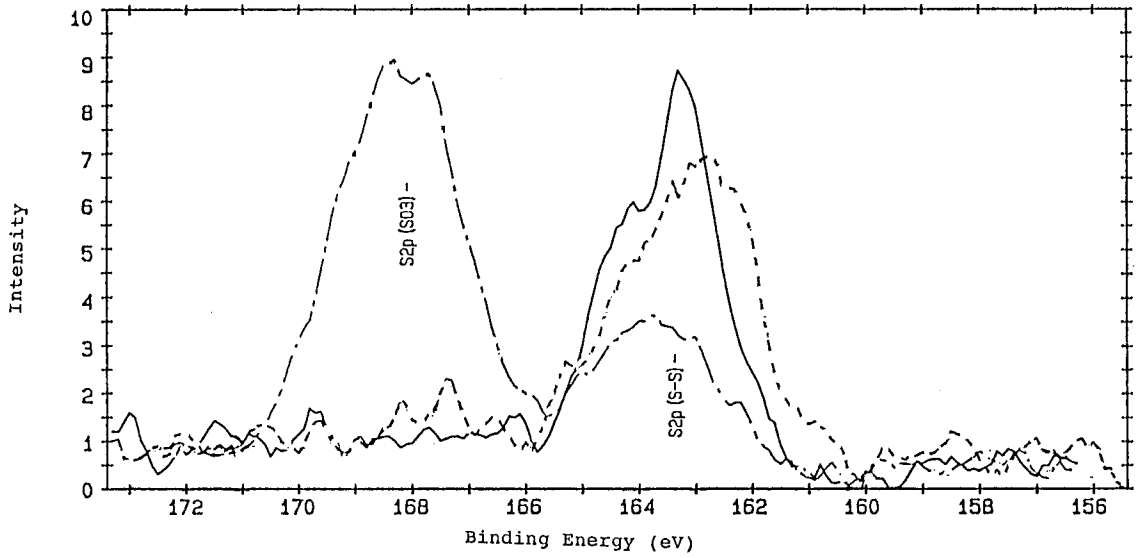

Figure 15. S $2p_{3/2}$ peaks of **1** (—), **3(PF$_6$)$_3$** (- - -), and **4** (— - —).

introduce any biased error, since the literature value of P(PF_6^-) $2p_{3/2}$ in $(Ph_3P)_3P^*F_6$ is 136.7 eV, compared to 135.9 eV in **3-(PF$_6$)$_3$**,[28] and the S($-SO_3^-$) $2p_{3/2}$ value of $NH_2C_6H_4SO_3H$ is 167.8 eV, which should be compared to 168.1 eV of **4** (Table 5). The relatively low Ru $3d_{5/2}$ and $3P_{3/2}$ binding energies of Ru(III) in the present compounds are therefore significant and seem to be caused by the strong π-donation of the S_2^{2-} ligand.[12] The S(S_2^{2-}) $2p_{3/2}$ binding energies in Figure 15 and in Table 5 are almost in the same range with those of other disulfide complexes i.e., 162.9−164.4 eV.[8] The binding energy of 162.7 eV for one-electron reduced **3(PF$_6$)$_3$** is slightly but significantly higher than those of the other two and might reflect that one additional electron is extensively delocalized onto the sulfur ligand. However, it may be a difference caused by the geometrical difference cis and trans of the RuSSRu core. All of the P $2p_{3/2}$, N 1s, and Cl $2p_{3/2}$ binding energies in Table 5 are normal.

Electronic State of the Mixed-Valent Core. Compound **[3]**$^{3+}$ shows several spectroscopic differences from other mixed-valent compounds. First, it lacks any intense absorption band in the longer-wavelength visible or near-IR spectral region, which is usually observed as a characteristic of mixed-valent compounds and which is not seen in the lower or higher isovalent forms. Second, **[3]**$^{3+}$ does not exhibit two metal core level photopeaks expected for Ru^{2+} and Ru^{3+} ions on the very short time scale (10^{-17} s) of the XPS experiment. These characteristics can be consistently understood by considering that in predominantly covalent systems such as **[RuSSRu]**$^{3+}$, assignment of metal oxidation states becomes less meaningful, and **[3]**$^{3+}$ is class III in the Robin and Day classification.[17]

The absence of an intense band typical of a mixed-valent compound can be explained as follows: if the ground state is completely valence-averaged (class III), there is no difference between the two metal oxidation states. It is reasonable that such a compound does not exhibit an intervalence metal-to-metal charge transfer band. It is also noteworthy that, in relation to the absence of an intervalence transition band, a dinuclear mixed-valent ruthenium(II,III) compound having an extensive π-delocalized bridging ligand with intensive metal−bridge orbital overlap, has an intense near-IR band close to that of the isovalent Ru(II,II) compound.[56] In such mixed-valent compounds, LMCT (or MLCT) and intervalence transitions (IT) are strongly coupled and both are almost inseparable, i.e., higher and lower isovalent forms and the mixed-valent form have almost identical λ_{max}. In the XPS of a such mixed-valent compound, only one photopeak is observed for each of Ru $3P_{1/2}$ and $3P_{3/2}$.[56] It is very intriguing to note that, in the resonance Raman spectrum of the Creutz−Taube mixed-valent ion, the

(56) Spreer, L. O.; Allan, C. B.; MacQueen, D. B.; Otvos, J. W.; Calvin, M. *J. Am. Chem. Soc.* **1994**, *116*, 2187.

Table 5. Electron Binding Energies (BE) and FWHM of the XPS Spectra[a]

		compound		
		1	**3(PF$_6$)$_3$**	**4**
Ru	$3d_{5/2}$			
	BE	281.0	281.0	281.4
	FWHM	1.3	1.3	2.0
	$3P_{3/2}$			
	BE	462.4	462.4	462.5
	FWHM	2.7	2.7	3.1
S(S_2)	$2P_{3/2}$			
	BE	163.2	162.7	163.4
	FWHM	2.1	2.7	2.2
S($-SO_3$)	$2P_{3/2}$			
	BE	nd	nd	168.1
	FWHM			2.7
P(TMP)[c]	$2P_{3/2}$			
	BE	133.1	133.0	133.1
	FWHM	1.7	2.0	2.0
P(PF_6)	$2P_{3/2}$			
	BE	nd	135.9	nd
	FWHM		1.5	
N	1S			
	BE	nd	399.6	399.9
	FWHM		1.3	1.4
Cl	$2P_{3/2}$			
	BE	197.9	nd	198.5
	FWHM	2.8		2.8

[a] BE and FWHM values are in eV. [b] nd = not determined. [c] TMP = $P(OMe)_3$.

symmetric stretching mode of pyrazine is strongly enhanced as well as the Ru−N stretching mode with medium strength when the IT band is irradiated.[57] The Raman band of the bridge ligand is the first piece of direct evidence that enables us to assign the IT band to the metal−bridge−metal three-site transition, which is different from a hitherto-believed metal−metal two-site one. In the resonance Raman spectrum of **3(PF$_6$)$_3$**, a strong ν(S−S) is enhanced while no or a very weak ν(Ru−S) is observed. In the mixed-valent compound **3(PF$_6$)$_3$**, although the absorption band is not very much different from those of Ru(III,III) compounds, it is more strongly coupled to a ν(S−S) stretching mode. A ν(S−S) resonance Raman band had been expected for a mixed-valent $Ru^{II}SSRu^{III}$ core,[15] but in actuality could not be observed, since such compounds had not been prepared.

The electrochemical parameters also support the assignment of **[3]**$^{3+}$ as a valence-averaged ($Ru^{2.5+}$,$Ru^{2.5+}$) compound. The large 1000-mV difference in the potentials for the formation of the mixed-valent and isovalent (Ru^{3+},Ru^{3+}) species of **[3]**$^{3+}$ corresponds to a comproportionation constant K_{com} of 8.0×10^{16}.

$$(Ru^{2+},Ru^{2+}) + (Ru^{3+},Ru^{3+}) \overset{K_{com}}{\rightleftharpoons} 2(Ru^{2+},Ru^{3+})$$

All of the above-mentioned facts suggest consistently that **[3]**$^{3+}$ is a class III compound with a valence-averaged ground state.

(57) Petrov, V.; Hupp, J. T.; Mottley, C.; Mann, L. C. *J. Am. Chem. Soc.* **1994**, *116*, 2171.

Appendix

In the matrix calculation, the electron configuration of low-spin d^5 is regarded as a one-hole state. It is assumed that a low-symmetry perturbation separates the one-hole real functions $\zeta(xy)$, $\eta(xz)$, and $\xi(yz)$, so that their energies are $(1/2)V$, $-(1/2)V$, and Δ, respectively. The g_x, g_y, and g_z are expressed as eqs 1−4,

$$g_x = 2[2AC - B^2 + kB(C - A)\sqrt{2}] \quad (1)$$

$$g_y = 2[2AC + B^2 + kB(C + A)\sqrt{2}] \quad (2)$$

$$g_z = 2[A^2 - B^2 + C^2 + k(A^2 - C^2)] \quad (3)$$

$$A^2 + B^2 + C^2 = 1 \quad (4)$$

where A, B, and C are normalization coefficients for the lowest Kramer doublet and k is an orbital reduction factor, which is a measure of the covalency of a metal−ligand bond. A knowledge of the g values enables these equations to be solved for A, B, C, and k. Then the secular eqs 5−7 are solvable for Δ/λ, V/λ, and E/λ.

$$((1/2)\lambda - E)A + (1/2)\lambda\sqrt{2}B + (1/2)VC = 0 \quad (5)$$

$$(1/2)\lambda\sqrt{2}A + (\Delta - E)B = 0 \quad (6)$$

$$(1/2)VA + (-(1/2)\lambda - E)C = 0 \quad (7)$$

The spin−orbit coupling constant λ is usually calculated by using the near-IR absorption band of the lowest transition.[29] However, since no absorption was observed in the near-IR region in the present study, λ was treated as an independent parameter and was determined together with other parameters.

Acknowledgment. The present research was supported by a Grant-in-Aid for Scientific Research on Priority Areas of "Activation of Small Molecules" (04241225) and of "Reactive Organometallics" (05236104) from the Ministry of Education, Science and Culture, Japan. We are greatly indebted to Prof. H. Takahashi of our Chemistry Department for his help in the measurement of the resonance Raman spectra.

Supporting Information Available: Details of the crystal data collection procedures for **1**, **2(CF$_3$SO$_3$)**, **3(PF$_6$)$_3$**, **4**, and **5**; anisotropic thermal parameters; interatomic distances and bond angles; the UV−vis spectral change during the reaction of **1** to **2**; the ORTEP drawing of the minor component of **[3]**$^{3+}$; the comparison of the core structures of **[3]**$^{3+}$ and **5**; details of the analytical method of the ESR spectrum; and $^{31}P\{^1H\}$ NMR spectra of **4** and **1** (47 pages). This material is contained in many libraries on microfiche, immediately follows this article in the microfilm version of the journal, can be ordered from the ACS, and can be downloaded from the Internet; see any current masthead page for ordering information and Internet access instructions.

JA950391V